Radiotherapy in a FLASH

Towards clinical translation of ultra-high dose rate electron therapy

Konradsson, Elise

2023

Total number of authors:
1

Radiotherapy in a FLASH

Towards clinical translation of ultra-high dose rate electron therapy

ELISE KONRADSSON
MEDICAL RADIATION PHYSICS
FACULTY OF SCIENCE | LUND UNIVERSITY

Radiotherapy in a FLASH

Radiotherapy in a FLASH

Towards clinical translation of ultra-high dose rate electron therapy

Elise Konradsson

LUND
UNIVERSITY

Organization		Document name:
Medical Radiation Physics Faculty of Science Lund University		DOCTORAL DISSERTATION
		Date of disputation: 2023-06-09
Author(s): Elise Konradsson		Sponsoring organization

Title and subtitle

Radiotherapy in a FLASH: Towards clinical translation of ultra-high dose rate electron therapy

Abstract

FLASH radiotherapy (FLASH-RT) is a promising new approach to radiotherapy that has the potential to transform the field. By administering radiation at ultra-high dose rates (UHDR) on a millisecond timescale, FLASH-RT may increase normal tissue tolerance compared to conventional radiotherapy while maintaining the anti-tumoral effect. However, the short treatment times present unique physical and technical challenges that must be resolved to ensure safe clinical implementation.

The overall aim of this thesis was to address some of these challenges and promote the clinical translation of electron FLASH-RT. Specifically, the studies included in this thesis aimed to develop, establish, and evaluate tools and procedures to measure, plan, and deliver the UHDR electron beam of a modified clinical linear accelerator.

In conventional radiotherapy, transmission chambers are used for beam monitoring during treatment delivery. In the first part of this thesis, we showed that the charge collection efficiency of the accelerator's built-in transmission chamber decreases substantially as the dose-per-pulse (DPP) increases. However, we also demonstrated that this issue could be overcome and that the operating range of the chamber could be extended up to the ultra-high DPP regime by adjusting its position, design, and operation. Our results suggest that a transmission chamber-based monitoring approach might also be employed in UHDR electron beams, which would make the procedure for FLASH-RT delivery similar to conventional delivery.

In the second part of this thesis, we established and evaluated dosimetric procedures for preclinical and clinical UHDR irradiations. Accurate delivery of the desired dose is critical to enable robust radiobiological studies that can help identify the biological mechanisms underlying the sparing effect of FLASH-RT and provide guidance in selecting beam parameters to test in clinical studies. We also demonstrated the feasibility of FLASH-RT in a clinical setting by initiating treatments of veterinary patients and conducting a dose-escalation trial in canine patients with spontaneously developed tumours. Finally, we also investigated a passive intensity-modulation technique with the aim of reducing the risk of radiation-induced side effects resulting from heterogeneous dose distributions in upcoming clinical trials. Our findings indicate that this technique, which is compatible with FLASH-RT delivery, can enhance the homogeneity of the dose distribution compared to utilizing an open electron beam.

In the work included in this thesis, we established and evaluated tools and procedures to enable accurate UHDR delivery in a preclinical and clinical setting, which is crucial for a safe path towards clinical translation of FLASH-RT.

Key words: radiotherapy, ultra-high dose rates, FLASH, dosimetry, translational research

Classification system and/or index terms (if any)

Supplementary bibliographical information	**Language:** English
ISSN and key title	**ISBN** 978-91-8039-666-0 (print) 978-91-8039-665-3 (pdf)

Recipient's notes	**Number of pages:** 79	Price
	Security classification	

Signature   Date 2023-05-05

Radiotherapy in a FLASH

Towards clinical translation of ultra-high dose rate electron therapy

Elise Konradsson

LUND
UNIVERSITY

Till Gun-Britt, Erland, Greta & Henry

Table of Contents

Abstract

FLASH radiotherapy (FLASH-RT) is a promising new approach to radiotherapy that has the potential to transform the field. By administering radiation at ultra-high dose rates (UHDR) on a millisecond timescale, FLASH-RT may increase normal tissue tolerance compared to conventional radiotherapy while maintaining the anti-tumoral effect. However, the short treatment times present unique physical and technical challenges that must be resolved to ensure safe clinical implementation.

The overall aim of this thesis was to address some of these challenges and promote the clinical translation of electron FLASH-RT. Specifically, the studies included in this thesis aimed to develop, establish, and evaluate tools and procedures to measure, plan, and deliver the UHDR electron beam of a modified clinical linear accelerator.

In conventional radiotherapy, transmission chambers are used for beam monitoring during treatment delivery. In the first part of this thesis, we showed that the charge collection efficiency of the accelerator's built-in transmission chamber decreases substantially as the dose-per-pulse (DPP) increases. However, we also demonstrated that this issue could be overcome and that the operating range of the chamber could be extended up to the ultra-high DPP regime by adjusting its position, design, and operation. Our results suggest that a transmission chamber-based monitoring approach might also be employed in UHDR electron beams, which would make the procedure for FLASH-RT delivery similar to conventional delivery.

In the second part of this thesis, we established and evaluated dosimetric procedures for preclinical and clinical UHDR irradiations. Accurate delivery of the desired dose is critical to enable robust radiobiological studies that can help identify the biological mechanisms underlying the sparing effect of FLASH-RT and provide guidance in selecting beam parameters to test in clinical studies. We also demonstrated the feasibility of FLASH-RT in a clinical setting by initiating treatments of veterinary patients and conducting a dose-escalation trial in canine patients with spontaneously developed tumours. Finally, we also investigated a passive intensity-modulation technique with the aim of reducing the risk of radiation-induced side effects resulting from heterogeneous dose distributions in upcoming clinical trials. Our findings indicate that this technique, which is compatible with FLASH-RT delivery, can enhance the homogeneity of the dose distribution compared to utilizing an open electron beam.

In the work included in this thesis, we established and evaluated tools and procedures to enable accurate UHDR delivery in a preclinical and clinical setting, which is crucial for a safe path towards clinical translation of FLASH-RT.

Populärvetenskaplig sammanfattning

Ungefär hälften av alla cancerpatienter genomgår strålbehandling, antingen som en enskild behandling eller i kombination med kirurgi och/eller medicinsk behandling. Vid strålbehandling används högenergetisk joniserande strålning för att bekämpa cancerceller. Strålningen orsakar skador på tumörcellernas DNA, men kan även skada friska celler. För att uppnå bästa möjliga behandlingseffekt med minsta möjliga biverkningar har forskning inom strålbehandling under flera decennier framgångsrikt eftersträvat två nyckelprinciper för att minimera stråldosen till frisk vävnad. Genom att dela upp behandlingen i flera fraktioner och krympa strålfältets marginaler kring tumören kan modern strålbehandling i många fall eliminera tumörer utan att orsaka oacceptabla biverkningar. Det finns dock fall där den stråldos som kan levereras till tumören begränsas av biverkningar som försämrar patientens livskvalitet. För att ytterligare minska biverkningar kan det krävas nya innovativa strategier som kan utnyttja den radiobiologiska skillnaden mellan tumör och frisk vävnad.

En sådan strategi är FLASH strålbehandling där stråldosen levereras med en ultra-hög doshastighet under bråkdelen av en sekund (ca 1000 gånger högre intensitet än vid vanlig strålbehandling). Den korta behandlingstiden skulle kunna minska effekten av patientrörelser under behandlingen, såsom andning, och därmed möjliggöra användning av snävare marginaler kring rörliga tumörer. Detta skulle resultera i en mer konform behandling med mindre frisk vävnad exponerad för höga stråldoser, vilket i sin tur skulle minska risken för strålningsinducerade biverkningar. Utöver detta har experimentella studier visat att denna typ av strålleverans under vissa förhållanden kan öka toleransen i den friska vävnaden med 10-50% jämfört med strålbehandling med konventionella doshastigheter utan att tumöreffekten påverkas.

FLASH har öppnat dörren för en ny strategi inom strålbehandling med potential att förbättra vården för cancerpatienter. Den korta strålleveransen kommer dock med unika fysikaliska och tekniska utmaningar som behöver lösas för att FLASH strålbehandling ska kunna implementeras och användas för patientbehandlingar i kliniken. Det övergripande syftet med denna avhandling var att adressera några av dessa utmaningar och främja den kliniska translationen av FLASH strålbehandling med elektroner. Mer specifikt syftade studierna i denna avhandling till att utveckla och utvärdera verktyg och procedurer anpassade för att mäta, planera och leverera den intensiva strålningen. Studierna är centrerade kring en klinisk linjäraccelerator som modifierats för att kunna leverera elektroner med ultra-höga doshastigheter.

Vid konventionell strålbehandling används vanligtvis en så kallad transmissions-kammare för att monitorera strålleveransen. Strålningen växelverkar med luften i

kammaren och producerar joner som samlas in och kan korreleras till den levererade dosen i en referensgeometri. Transmissions-kammarens insamlingseffektivitet har dock visat sig försämras avsevärt när de exponeras för strålning med ultra-höga doshastigheter, vilket påverkar dess funktion. I avhandlingens första två studier demonstrerade vi hur detta problem kan hanteras och delvis övervinnas genom att justera transmissions-kammarens placering, elektrodavstånd och pålagda spänning.

I den tredje och fjärde studien etablerade vi dosimetriska procedurer för bestrålning med ultra-höga doshastigheter vid experimentella och veterinärkliniska försök. Noggranna dosimetriska procedurer vid experimentell bestrålning är kritiska för att kunna utföra högkvalitativa radiobiologiska studier som kan hjälpa oss att förstå de biologiska mekanismerna som ligger bakom den sparande effekten som observerats vid ultra-höga doshastigheter och vägleda oss i valet av leveransparametrar att testa i kliniska studier. I den fjärde studien demonstrerade vi även genomförbarheten av klinisk FLASH strålbehandling i form av en doseskaleringsstudie med veterinära hundpatienter med spontant utvecklade tumörer.

Vid dagens strålbehandling moduleras strålens intensitet under behandlingen för att skapa en jämn och konform dos till tumören. På grund av den korta behandlingstiden vid FLASH strålbehandling kan inte nuvarande intensitetsmodulerande teknik med rörliga delar användas. I den femte studien utvärderade vi potentialen av en alternativ teknik där strålens intensitet moduleras med passiva metallstift som blockerar delar av strålen i ett optimerat mönster. Förhoppningen är att använda denna metod i framtida kliniska försök för att minska risken för strålningsinducerade biverkningar orsakade av en ojämn fördelningen av dosen.

I studierna inkluderade i denna avhandling etablerade och utvärderade vi verktyg och procedurer för noggrann leverans av strålning med ultra-höga dosrater, både vid experimentella och kliniska försök, vilket är kritiskt för att säkra en klinisk translation av FLASH strålbehandling.

Original Papers

This thesis is based on the following papers, which are referred to by Roman numerals:

I. **Correction for ion recombination in a built-in monitor chamber of a clinical linear accelerator at ultra-high dose rates**
    Konradsson E, Ceberg C, Lempart M, Blad B, Bäck S, Knöös T and Petersson K
    Radiation Research. 2020;194(6):580-586.

II. **Reconfiguring a plane-parallel transmission ionization chamber to extend the operating range into the ultra-high dose-per-pulse regime**
    Konradsson E, Ericsson Szecsenyi R, Wahlqvist P, Thoft A, Blad B, Bäck S, Ceberg C and Petersson K
    Manuscript submitted to *Physics in Medicine & Biology* (2023).

III. **Development of dosimetric procedures for experimental ultra-high dose rate irradiation at a clinical linear accelerator**
    Konradsson E, Petersson K, Adrian G, Lempart M, Blad B, Ceberg S, Knöös T, Bäck S and Ceberg C
    Journal of Physics: Conference Series. 2022;2167.

IV. **Establishment and initial experience of clinical FLASH radiotherapy in canine cancer patients**
    Konradsson E*, Arendt ML*, Bastholm Jensen K, Børresen B, Hansen A. E, Bäck S, Kristensen A T, Munck af Rosenschöld P, Ceberg C and Petersson K
    Frontiers in Oncology. 2021 May 13;11:658004. * Shared first authorship

V. **Evaluation of intensity-modulated electron FLASH radiotherapy in a clinical setting**
    Konradsson E, Ericsson Szecsenyi R, Adrian G, Coskun M, Børresen B, Arendt ML, Erhart K, Petersson K and Ceberg C
    Manuscript submitted to *Medical Physics* (2023).

List of contributions

Below is a summary of my contributions to each of the original papers:

I.   I took part in the study design and the development of the methodology. I planned and performed all measurements and analyzed the data. I drafted the manuscript and was the main and corresponding author.

II.   I contributed to the scientific question and the development of the methodology. I planned and performed all measurements and analyzed the data. I drafted the manuscript and was the main and corresponding author

III.   I contributed to the scientific question. I took part in the development of setups and procedures. I performed all measurements and analyzed the data. I drafted the proceeding and was the main and corresponding author.

IV.   I took part in the development of the workflow. I was responsible for the dosimetry and the delivery of the treatments. I performed the measurements and analyzed the data. I drafted the manuscript with help from Maja L. Arendt and we shared the first authorship.

V.   I participated in the study design and performed the treatment planning and data collection. I analyzed the data, drafted the manuscript, and was the main author.

Related papers not included in this thesis

- Adrian G, <u>Konradsson E</u>, Lempart M, Bäck S, Ceberg C and Petersson K. **The FLASH effect depends on oxygen concentration.** *The British Journal of Radiology.* 2020;93 (1106).

- Adrian G, <u>Konradsson E</u>, Beyer S, Wittrup A, Butterworth K, McMahon S, Ghita M, Petersson K and Ceberg C. **Cancer cells can exhibit a sparing FLASH effect at low doses under normoxic in vitro-conditions.** *Frontiers in Oncology.* 2021;11.

- <u>Konradsson E</u>, Liljedahl E, Gustafsson E, Adrian G, Beyer S, Ehsaan Ilaahi S, Petersson K, Ceberg C and Nittby Redebrandt H. **Comparative long-term tumor control for hypofractionated FLASH vs. conventional radiation therapy in an immunocompetent rat glioma model.** *Advances in Radiation Oncology.* 2022;7(6).

- Liljedahl E, <u>Konradsson E,</u> Gustafsson E, Förnvik Jonsson K, Olofsson J.K, Ceberg C and Nittby Redebrandt H. **Long-term anti-tumor effects following both conventional radiotherapy and FLASH in glioblastoma.** *Scientific Reports.* 2022;12(1).

- Mannerberg A, <u>Konradsson E</u>, Kügele M, Edvardsson A, Kadhim M, Ceberg C, Petersson K, Thomasson H-M, Arendt ML, Børresen B, Bastholm Jensen K and Ceberg S. **Surface guided electron FLASH radiotherapy for canine cancer patients.** *Medical Physics.* 2023.

- Børresen B, Arendt ML, <u>Konradsson E</u>, Bastholm Jensen K, Hansen A. E, Bäck S, Kristensen A T, Munck af Rosenschöld P, Ceberg C and Petersson K. **Toxicity and efficacy of single-fraction high dose FLASH radiotherapy in a cohort of dogs with spontaneous malignant oral tumors**. Submitted to *International Journal of Radiation Oncology, Biology, Physics* 2023.

- Brus A, <u>Konradsson E</u>, Eriksson S, Adrian G, Carneiro A, Petersson K, Hansen A.E, Andresen T.L and Ceberg C. **Comparison of the anti-tumor effect and immune-biological response in the tumor microenvironment after FLASH or conventional electron irradiation.** Submitted to *Radiation Oncology* 2023.

Abbreviations

FLASH-RT	FLASH radiotherapy
UHDR	ultra-high dose rate
TCP	tumour control probability
NTCP	normal tissue complication probability
CONV	conventional dose rates
CONV-RT	conventional radiotherapy
PRF	pulse repetition frequency
DPP	dose-per-pulse
SSD	source-to-surface distance
IAEA	International Atomic Energy Agency
TVA	two-voltage-analysis
TLD	thermoluminescent dosimeters
MU	monitor units
BCT	beam current transformer
PFN	pulse forming network
SC	squamous cell carcinoma
IORT	intraoperative radiotherapy
TPS	treatment planning system
PTV	planning target volume
MLC	multi-leaf collimator
CI	conformity index
HI	homogeneity index

Introduction

Radiotherapy is one of the cornerstones of modern cancer oncology, with more than half of all cancer patients receiving curative or palliative radiotherapy as part of their treatment (1). External beam radiotherapy is mainly a local treatment in which high-energy radiation beams are produced, often by a medical linear accelerator, and directed at the tumour. The accelerator generates electrons that can be used directly or converted into X-rays before they reach the patient. The goal and constant challenge of radiotherapy is to deliver a high enough radiation dose to the tumour to eliminate cancer cells while minimizing the exposure of healthy normal tissue. The range of radiation doses that maximizes the tumour control probability (TCP) and minimizes the normal tissue complication probability (NTCP) is called the therapeutic window. The therapeutic window is determined by several factors, such as the tumour type and the sensitivity of the surrounding healthy tissues to radiation.

For decades, radiotherapy research has successfully pursued two key principles to enhance the therapeutic window: dose fractionation and spatial conformity. A fractionated treatment regimen, in which the total dose is divided into smaller dose fractions and administered over several weeks, is part of the standard of care practice to protect normal tissues from radiation-induced damage. Such a treatment regimen takes advantage of the fact that healthy tissue recovers more efficiently from radiation-induced damage than tumours. To further widen the therapeutic window, the volume of the exposed normal tissue can be reduced by shrinking the margins of the radiation field around the tumour. Several advanced techniques, such as intensity-modulated radiotherapy, stereotactic radiotherapy, image-guided radiotherapy, and volumetric modulated arc therapy, have been successfully introduced into clinical practice to improve 3D conformity of the dose delivery. However, tumour radioresistance and normal tissue toxicity still pose major challenges to treatment efficacy, and further improvements in spatial dose conformity may be limited by factors such as the physical properties and geometry of the radiation beam, the accuracy of patient positioning and image guidance, as well as the ability to manage the patient motion during treatment (i.e., intrafractional motions). To further expand the therapeutic window, new innovative strategies that take advantage of the radiobiological difference between tumours and normal tissue may be required.

In recent years, a rediscovered concept has emerged as a modality with the potential to transform the traditional radiotherapy paradigm of delivering the treatment in daily fractions over several weeks. This concept, known as FLASH radiotherapy (FLASH-RT), is characterized by an ultra-high dose rate (UHDR) delivery (2,3). The short beam-on time (on the millisecond timescale) associated with this type of delivery can eliminate the effects of intrafractional motion during treatment and enable tighter treatment margins for moving targets. Tighter treatment margins would result in a more conformal treatment with less healthy tissue exposed to high radiation doses, which could, in turn, reduce the risk of radiation-induced side effects. Additionally, and even more interestingly, preclinical studies have shown that under certain conditions, UHDR delivery may increase the normal tissue tolerance dose for a given endpoint by 10-50% compared to radiotherapy with conventional dose rates (CONV) on the order of Gy/minute, without compromising the anti-tumoral effect (3–7). In cancer types where tumour control can already be achieved with conventional radiotherapy (CONV-RT), this increased tolerance could either be exploited to reduce normal tissue complications or to reduce the number of fractions (i.e., hypofractionated treatment) with remained total dose and tumour effect. The increased tolerance could also be exploited to escalate the dose to radiosensitive cancers that are difficult to cure without increasing the toxicity.

FLASH-RT has opened the door to a new strategy in radiotherapy with the vision of improved clinical outcomes for multiple cancer patient groups and, if the number of fractions can be reduced, an increased capacity for radiotherapy departments and reduced waiting lists. However, to enable the clinical implementation of FLASH-RT, careful interdisciplinary research is required to better understand the physical parameters and biological mechanisms that trigger the protective effect in normal tissues while preserving therapeutic efficacy. FLASH-RT is still in the early stages of development and presents many unique challenges that need to be resolved before large-scale deployment of the technique can be considered. This includes enabling treatment machines to deliver radiotherapy at UHDR in a clinical setting with high safety and with good dosimetric and geometric accuracy, and establishing robust procedures for preclinical and clinical FLASH delivery.

Research aims

The overall aim of the work in this thesis was to promote the clinical translation of electron FLASH-RT.

The first aim was to investigate the potential for transmission chamber-based beam monitoring of an UHDR electron beam. The specific aims of this part were:

- To investigate whether the built-in transmission chamber of a clinical linear accelerator can be useful for real-time dosimetry at UHDR (**Paper I**)

- To study the potential to increase the charge collection efficiency of a transmission chamber by modifying its position, design, and operation (**Paper II**)

The second aim was to establish and evaluate dosimetric procedures and to perform preclinical and clinical FLASH irradiations. The specific aims of this part were:

- To establish experimental setups and dosimetric procedures for experimental FLASH irradiation (**Paper III**)

- To establish a clinical workflow for FLASH-RT in canine cancer patients and share initial treatment experiences (**Paper IV**)

- To evaluate the clinical possibilities of intensity-modulated electron FLASH-RT for improved dose distribution (**Paper V**)

Background

History of ultra-high dose rate (FLASH) radiotherapy

The first report of an altered biological response after UHDR radiation dates back to 1959, when Dewey and Boag (after encouragement from Dr. L. H. Gray) observed that bacteria were less radiosensitive to high-dose single μs electron pulses than when exposed to the same dose with CONV (6 Gy/min) X-ray irradiation (8) (Figure 1). A sparing effect on mammalian cells was first demonstrated by Town *et al.* 1967 after single pulse delivery with an average dose rate of ~10^7 Gy/s (9), and in 1982 Hendry *et al.* demonstrated induced resistance to epithelial necrosis in the tail of mice at average dose rates of ~10^3 Gy/s (10). Several other studies from the same period observed similar phenomena in different biological systems (11–13). In contrast, some authors reported no difference in biological effect in mammalian cells exposed to UHDR compared to CONV irradiation (14–16). The conflicting results might be explained by the cells being cultured and irradiated under atmospheric oxygen concentration which is not representative of the oxygen concentrations found *in vivo*. However, Zackrisson *et al.* found no significant differences in cell survival between UHDR (~$4x10^2$ Gy/s) and CONV (~6 Gy/min) irradiation when using a 50 MeV beam to irradiate a fibroblast V-79 cell line under both oxic and anoxic conditions (16). These early observations did not lead to further advances at this time, mainly because 1) it was believed that the total dose required to achieve a sparing effect would be too high to be clinically applicable, 2) the potential sparing effect on tumours, and 3) clinical UHDR sources were not widely available at the time.

A renewed interest in radiotherapy using UHDR was sparked in 2014, when Favaudon *et al.* published a comparative study in which a single dose of radiation was delivered to the thorax of mice with either FLASH (≥40 Gy/s) or CONV (≤1.8 Gy/min) irradiation (2). A single dose of 17 Gy FLASH (4.5 MeV) resulted in a dramatically lower degree of radiation-induced pulmonary fibrosis compared to 17 Gy CONV (4.5 MeV). After increasing the FLASH dose to 30 Gy, the side effects became significant and similar to the CONV 17 Gy group. In the same publication,

two different xenograft models (breast cancer HBCx-12A and head and neck cancer Hep-2) growing subcutaneously in nude mice were investigated in terms of tumour growth, showing that FLASH and CONV were equally effective in inducing tumour growth delay (2). The sparing of normal tissue with maintained tumour response after FLASH compared to CONV irradiation has been termed the 'FLASH effect'. In 2017, Montay-Gruel *et al*. reported on neurocognitive function after 10 Gy whole-brain electron irradiation delivered at a range of average dose rates from 0.1 Gy/s to 10^6 Gy/s (17). Using a novel object recognition test, the authors showed that working memory was fully preserved at average dose rates of ≥100 Gy/s, while no notable protection of memory function was observed at average dose rates of ≤20 Gy/s. To date, the normal tissue sparing effect as well as the similar anti-tumour effect have both been replicated in several preclinical models for different types of particles (3–6,18–20). Additionally, studies in larger animals have been conducted to investigate FLASH-RT in scenarios applicable to human patients (21–23).
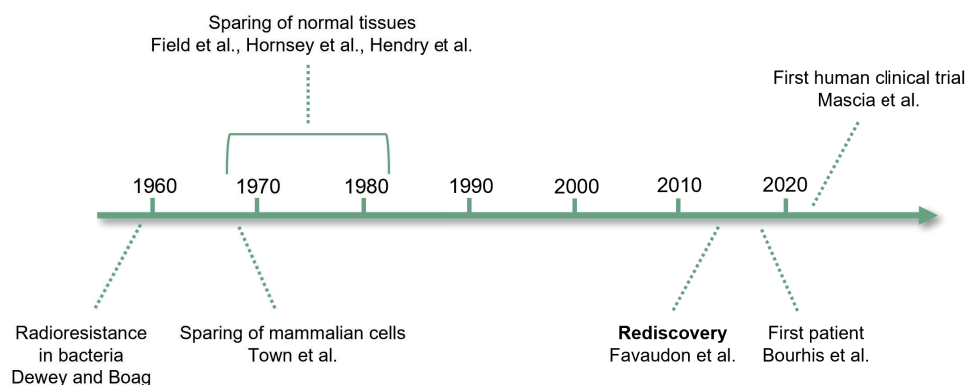
Figure 1: Timeline describing the history of ultra-high dose rate (UHDR) irradiation and FLASH radiotherapy.

In 2019, the first human patient treated with FLASH-RT was reported (24). The patient was a 75-year-old male diagnosed with CD30+ cutaneous T-cell lymphoma in 1999 and had been treated with CONV-RT at >100 occasions with good treatment effect but poor skin tolerance. After receiving a single fraction of 15 Gy FLASH-RT (167 Gy/s) delivered in 10 electron pulses over a total treatment time of 90 ms, a complete tumour response was achieved 36 days post-treatment. The observed skin toxicity was limited to grade 1 epithelitis and grade 1 oedema, which were considered to be substantially milder than for previous CONV-RT. In 2021, the same patient

was treated for two distinct tumours on the same day with 15 Gy FLASH-RT (166 Gy/s) and 15 Gy CONV-RT (0.08 Gy/s), respectively (25). In a direct comparison, no difference was found between the two treatments, neither with regard to acute reactions, late effects after 2 years, nor tumour control. More recently, the results of the first clinical human FLASH trial, FAST-01, were published (26). In this trial, ten patients with symptomatic bone metastases in the extremities were palliatively treated with 8 Gy proton FLASH (≥40 Gy/s) with desired therapeutic benefit.

Given the *in vivo* evidence of a FLASH effect under certain conditions, there appears to be a potential for an expanded therapeutic window with FLASH that may be exploited in the radiotherapy practice (Figure 2). The feasibility of the treatment of the first patient as well as the FAST-01 trial further demonstrate the potential for a clinical translation of FLASH-RT (24–26).
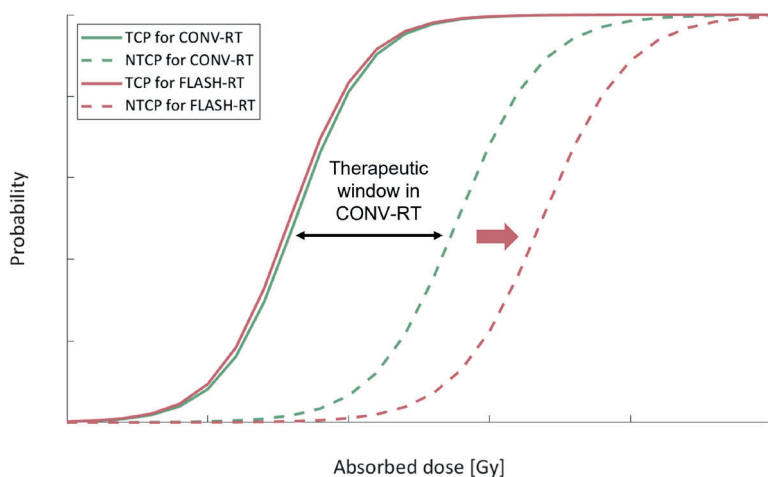
Figure 2 : Illustration of the therapeutic window, i.e., the separation between the tumour control probability (TCP) curve and normal tissue complication probability (NTCP) curve, for conventional radiotherapy (CONV-RT, green) and FLASH radiotherapy (FLASH-RT, pink). With a suggested dose-modifying factor of 10-50%, FLASH-RT has the potential to widen the therapeutic window as compared to CONV-RT.

Ultra-high dose rate physics and dosimetry

UHDR radiotherapy involves administering the radiation dose at dose rates several orders of magnitude higher than those used in CONV-RT. These extreme conditions bring new technical challenges, and one of the main barriers for a clinical

implementation of FLASH-RT is associated with technology and dosimetry at UHDR.

Beam parameters

The FLASH studies performed so far have involved different types of particles (electrons, protons, X-rays, heavy ions) and radiation sources (dedicated electron accelerators, medical linear accelerators, cyclotrons, synchrotrons). These machines all produce pulsed radiation beams, although the pulse structure (such as the pulse length and pulse repetition frequency (PRF)) can differ substantially, which may be part of the explanation for the variations in the magnitude of the observed (or not observed) normal tissue sparing between different studies. In the early years of FLASH research, it was suggested that the average dose rate was the main parameter for modulating the sparing effect. However, with the availability of more preclinical data, several authors have reviewed the key temporal beam parameters for observing a FLASH sparing effect (3,6,7,24,27). They suggest that not only the average dose rate, but also the pulse dose rate, dose-per-pulse (DPP), PRF and total delivery time may be important. In addition, the dose per fraction seem to play an important role (20). It becomes clear that the term 'dose rate' needs to be specified more precisely, and in order to allow a robust comparison between studies it has been suggested that authors should provide specific information about the beam and pulse characteristics (7). The important temporal beam parameters are described in Table 1 and Figure 3.

Table 1. Important temporal beam parameters and their respective common values for conventional (CONV) electron radiotherapy and for FLASH electron radiotherapy from a linear accelerator.

Beam parameter	Description	CONV	FLASH
Average dose rate ($\dot{D}$)	Mean dose-rate for multi-pulse delivery	~10^0-10^1 Gy/min	≥30-40 Gy/s
Pulse dose rate ($\dot{D}_p$)	Dose-rate within a single pulse	~10^2 Gy/s	≥10^5-10^6 Gy/s
Dose-per-pulse (DPP)	Dose delivered in a single pulse	~10^{-4}-10^{-3} Gy	≥1 Gy
Pulse repetition frequency (PRF)	Number of pulses delivered per unit time	~10^2 Hz	~10^2 Hz
Pulse duration (w)	Time for delivery of a single pulse	few μs	few μs
Number of pulses (n)	Number of pulses delivered during one fraction	~10^3-10^4	<20
Total delivery time (t)	Irradiation time from start of first pulse to the end of the last pulse	~10^0-10^1 min	≤0.1-0.2 s
Time between pulses (t_n)	Time from end of one pulse to start of next pulse	~ms	~ms
Fraction dose (D)	Total dose for a single fraction	~2 Gy	≥5-10 Gy

Data on how the values of these parameters affect the radiobiological effect are still limited. Further studies are needed to narrow down the options and set requirements for the radiation sources to be used. However, according to current understanding, the observation of a FLASH effect generally requires average dose rates of ≥30-40 Gy/s, a total irradiation time of <200 ms, and faction doses of ≥5-10 Gy (3,4,6,7,27).

$$DPP = \dot{D}_p \times w$$
$$D = DPP \times n$$
$$\dot{D} = D/t$$
$$PRF = 1/t_n$$
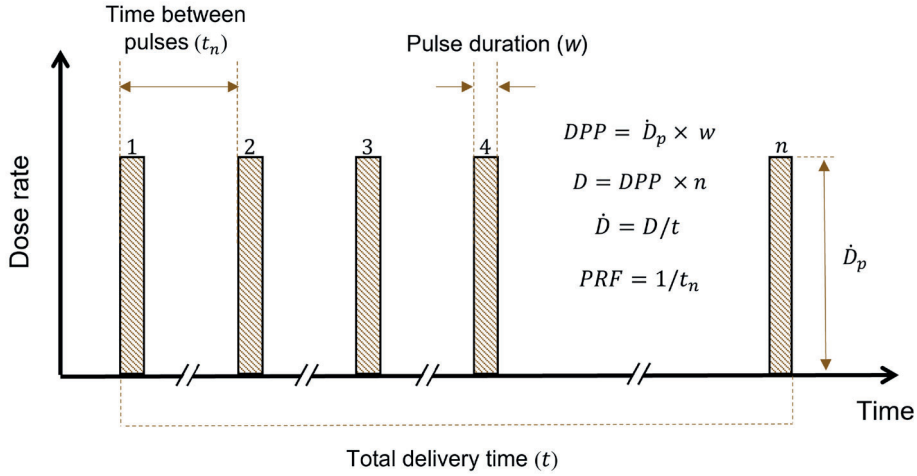
Figure 3: Terminology and pulse structure of a pulsed electron beam. The figure is adapted from (3).

Radiation sources

The majority of radiotherapy treatments are delivered with high-energy X-rays generated by clinical linear accelerators. These beams are widely available and have a penetration depth that can reach deep-seated tumours. However, the beam parameter requirements for FLASH described above are difficult to meet due to the ineffective generation of clinical high-energy X-rays through the bremsstrahlung conversion process. Consequently, FLASH studies have so far been performed with alternative radiation sources capable of producing UHDR beams.

Electrons

Initial FLASH studies were performed with electron beams generated by dedicated research linear accelerators, namely the 4.5 MeV Kinetron (CGR-MeV, Paris, France) (2,28) and the 6 MeV Oriatron eRT6 (PMB-Alcen, Peynier, France) (29,30). The

advantage of these accelerators lies in the wide range of achievable pulse structures, which make them suitable for preclinical FLASH studies.

In 2017, researchers from Stanford University School of Medicine presented an approach to using a clinical linear accelerator (Clinac 21EX, Varian Medical Systems, Palo Alto, CA, USA) for FLASH irradiation of small animals (31). By positioning the subject in the mirror position in the head of the gantry, an average dose rate of 220 Gy/s was achieved, with a field diameter of ~4 cm receiving >90% of the dose. This approach inspired other researchers to modify linacs and enable FLASH research at their respective institutions. In 2019, one of the clinical Elekta linear accelerators (ELEKTA Precise, Stockholm, Sweden) at Skåne University Hospital in Lund was modified by reconfiguring the beam control parameters to deliver a 10 MeV electron beam at an average dose rate of >120 Gy/s, >250 Gy/s, and >1000 Gy/s at the cross-hair foil, multi-leaf collimator (MLC), and wedge position, respectively (32). This accelerator was used throughout the work in this thesis (**Papers I-V**). More details about this accelerator are presented in the next chapter. A group at Dartmouth College and Dartmouth-Hitchcock Medical Center modified a Varian Clinac 2100 C/D (Varian Medical Systems, Palo Alto, CA, USA) (33). With the jaws completely open, i.e., a field size of 40x40 cm^2 at isocenter distance, they could achieve average dose rates >300 Gy/s (0.86 Gy per pulse at 360 Hz) at a source-to-surface distance (SSD) of 100 cm. Furthermore, a dedicated intraoperative mobile linac accelerator (Novac7, SIT, Aprilia, Italy) was converted into a FLASH-enabled device capable of delivering average dose rates of up to 540 Gy/s, i.e., 18 Gy per pulse with a PRF of 30 Hz (34). This machine was later developed into the ElectronFlash system (35,36).

More recently, medical linear accelerators designed for UHDR delivery of electron beams have been developed and commissioned, such as the Mobetron by IntraOp and the FLASHknife by PMB-Alcen (now THERYQ) (29,37). The Mobetron was commissioned for 6 MeV and 9 MeV nominal energies. With an SSD of 37.3 cm, the average dose rate was about 300 Gy/s, the maximum DPP was 3-3.3 Gy, and the treatment depth (R90) was 2-2.5 cm with a maximum field size of 6 cm (37). The FLASHknife is a further development of the Oriatron with an energy of 5-6 MeV. For this system, the maximum DPP is 10 Gy and the PRF can be adjusted between 5 and 200 Hz. With an SSD of 100 cm, the FLASHknife can deliver field sizes between 1.6 and 20 cm with a treatment depth (R80) of 1.8-2.3 cm (29).

Since the initial studies on FLASH-RT were carried out using high-energy electrons, and the necessary setups are already in place, it is convenient to conduct a proof-of-concept for clinical FLASH-RT in humans in this setting first, which can later be advanced to other beam qualities that allow for treatment of deep-seated tumours. In fact, this is already ongoing using the Mobetron (38,39).

Protons

Due to the limited practical range of the beams, FLASH-RT using medium- and high-energy electrons is restricted to preclinical studies and superficial, subcutenaous or intraoperative treatments of higher mammals, domestic animals, and humans. However, the protective effect on normal tissues with FLASH-RT compared to CONV-RT has also been observed with protons. Clinical protons beams (~230-250 MeV) have advantageous physical properties, such as increased tissue penetration compared to high-energy electrons, and a finite range that can be exploited to produce a superior dose distribution with a high dose in a spread-out Bragg Peak and a low dose in front of and behind the target. Most modern clinical proton beams, with some adjustments in operating parameters, can achieve the average dose rates required to obtain FLASH dose rates in individual spots. However, different accelerator technologies are associated with different time structures. Several experimental setups for proton FLASH have been established (40–44). Most modern proton therapy facilities are operated with pencil beam scanning, which involves a deadtime between spots, an energy shift between each scanning layer, and a variation of the beam current at each spot. All of these factors reduce the average dose rate, making it difficult to irradiate large volumes without falling below the dose rate requirements for FLASH (45). In order to make these systems FLASH-capable for clinically relevant volumes, developments to increase the speed of the delivery are required. Hybrid approaches have been proposed using scanned beams together with patient-specific range modulators (46). A detailed description of the technical challenges for proton FLASH-RT can be found in a review article by Jolly *et al.* (45).

Nonetheless, the first clinical human trial of FLASH-RT was recently performed at the Cincinnati Children's/UC Health Proton Therapy Center using a FLASH-enabled proton therapy system (ProBeam, Varian Medical Systems) with a 250 MeV transmission beam (26). This system can deliver clinical field sizes with a nominal isocenter dose rate of 60 Gy/s (26). The limitation of transmission beams compared to clinically used proton beams is the lack of normal tissue sparing provided by the presence of the spread-out Bragg peak.

Photons

Although UHDR X-ray beams cannot be generated with clinical linear accelerators, other X-ray sources have been used for preclinical FLASH research (47,48). Montay-Gruel *et al.* observed sparing of normal brain injuries in mice after X-ray irradiation generated using a synchrotron light source (48). The dose was delivered by scanning the animals through a 50 μm slice, resulting in an average dose rate of 37 Gy/s. Gao *et al.* reported a FLASH effect in tumour-bearing mice using a MV photon beam

produced by a superconducting linear accelerator (PARTNER platform at CTFEL) (47). It has also been proposed to use conventional X-ray tubes for FLASH irradiation, although these beams may have an even more limited range than high-energy electrons (49). An interesting solution for future UHDR research is known as the PHASER (Pluridirectional High-energy Agile Scanning Electronic Radiotherapy) and was proposed in 2019 (50). The PHASER will include an array of linacs, each using an electron beam scanned on a stationary target and a collimator array to produce an intensity-modulated X-ray beam. The PHASER is designed to provide ultra-rapid image-guided radiotherapy delivery in a compact and economical platform with better RF power efficiency, higher beam current, and lower manufacturing costs compared to current linacs (50). Although the development of the PHASER is a long-term project relying on many new technical innovations, it could be the preferred source for clinical FLASH-RT in the future.

Very high energy electrons

Another option to treat deep-seated sites with FLASH-RT is to use very high energy electrons in the range of 50-250 MeV. The advantages of very high energy electron beams compared to X-rays and proton beams are the sharp penumbra and their insensitivity to tissue inhomogeneities (51,52). In the 90s, the MM50 Racetrack microtron was used in some clinics to treat patients with a 50 MeV electron beam (53). Current medical linear accelerators cannot produce these high energy beams, but laser-driven accelerators such as plasma accelerators or dielectric laser accelerators can (54,55). Unfortunately, laser-driven accelerators are not yet suitable for radiotherapy due to their large size, small beam sizes, and stability issues. Another type of accelerator capable of performing conformal very high energy electron FLASH-RT using accelerating gradients of 100 MeV/m is currently being developed in a collaboration between researchers at CHUV Lausanne University Hospital and CERN.

Dosimetry tools

The purpose of proper dosimetry in clinical radiotherapy is to ensure that the patient receives the prescribed dose. In the preclinical setting, accurate dosimetry is crucial for high-quality experiments that can predict response to radiation and inform clinical treatment schedules. However, dosimetry in UHDR conditions is challenging, and many of the dosimetry tools routinely used in CONV-RT fail in performance when used in these beams. Therefore, before a clinical implementation of FLASH-RT, new innovative dosimetry methods capable of handling the intense dose delivery needs to be developed. To ensure this, a further understanding of the potential and limitations

of different detector types under UHDR conditions is required. At this time, there is no code of practice on how to measure absorbed dose under these extreme conditions. A workgroup named UHDpulse was established with the aim of providing the metrological tools needed to establish traceability in absorbed dose measurements for particle beams with ultra-high DPP (56). The detectors are preferably already available or can be easily implemented on existing accelerator facilities. As with the detectors used in CONV-RT, tissue equivalence, energy independence, and high spatial resolution are advantageous properties. Some additional properties that make a detector suitable for dosimetry in UHDR beams are dose rate independence (both average dose rate and pulse dose rate) and high temporal resolution.

Ionization chambers

Real-time dose measurements in CONV-RT are frequently performed using ionization chambers, which are also the primary tools recommended by the International Atomic Energy Agency (IAEA) in the Technical Report Series (TRS) 398 describing the code of practice for dose determination in external beam radiotherapy (57). The principle of ionization chambers is based on two electrodes with an applied voltage to generate an electric field. Upon exposure to ionizing radiation, molecules in the chamber gas are ionized and excited, creating ion pairs in random thermal motion that are collected by the electrodes, and the charge can then be used to quantify the absorbed dose. The polarizing voltage applied over the chamber is typically high enough to collect all the produced ion pairs. However, at high dose rates, ion pairs may recombine before being collected by the electrodes. After a certain threshold of produced charge per unit time, the charge collection efficiency decreases with increasing DPP (30,58).

A commercial ionization chamber that can collect ion pairs at DPP values up to 5 mGy is the Advances Markus chamber (PTW, GmbH, Freiburg, Germany). If this is not sufficient to collect all ion pairs, the remaining loss in efficiency due to ion recombination can usually be corrected for using theoretical models from Boag *et al.* (59). However, for the UHDR beams used in FLASH-RT (DPP values in the order of Gy), these models are insufficient. Small chambers (which are not recommended for reference dosimetry in currently existing dosimetry protocols) have been shown to require smaller recombination correction factors compared to larger chambers (60,61). This is consistent with Boag's theories, which state that ion recombination is proportional to the distance between the electrodes and inversely proportional to the strength of the electric field (59,62). The 31014 PinPoint chamber (PTW, GmbH, Freiburg, Germany) has been used in synchrotron X-ray FLASH studies (48,63). Other groups have successfully used small-size ionization chambers in UHDR proton

beams (40,64). It should be noted that for this type of proton and synchrotron beams, the PRF is around 100 MHz, which is considerably higher than for typical electron beams produced by linear accelerators, and consequently, the DPP is considerably smaller.

In the recent literature, advances have been made in developing plane-parallel ionization chambers with minimal electrode spacing to make them suitable for UHDR beams (65,66). Gomez *et al.* simulated and subsequently designed an ultra-thin plane-parallel ionization chamber with an electrode distance of 0.25 mm (66), which could be operated with recombination effects similar to those in CONV beams (<1%) for DPP values up to 7.5 Gy per pulse. This finding was consistent with a recent study by Kranzer *et al.*, where the effect of reduced electrode distance in combination with increased chamber voltage was studied (67). A different approach was used by Di Martino *et al.* when they conceptualized an ionization chamber filled with nobel Argon gas (68). In theory, this design allows for a linear response of the chamber up to 40 Gy per pulse. In **Papers I** and **II**, the ion recombination effects in large size plane-parallel transmission chambers were investigated. Additionally, the response of a Baldwin-Farmer type ionization chamber placed in the bremsstrahlung tail of the UHDR electron beam was investigated in **Paper I**. The same Baldwin-Farmer type chamber was also used for relative output measurements in **Papers III and IV**.

Ion recombination correction models

There are two types of recombination effects in ionization chambers: initial recombination and volume (general) recombination. Initial recombination occurs between ions generated in the same ionization track. Therefore, this process is most pronounced for heavy ions with densely ionized particle tracks and is generally less than 0.2% for other beams (57). The initial recombination is independent of the ionization current, i.e., the dose rate. Volume recombination occurs when ions generated in different ionization tracks recombine, and this process is dose rate dependent.

For CONV irradiation it is recommended by the TRS 398 to derive a recombination correction factor, k_s, to correct for the lack of complete ion collection due to volume recombination effects using the two-voltage analysis (TVA) method (57,69):

$$k_s = a_0 + a_1 \left(\frac{M_1}{M_2}\right) + a_2 \left(\frac{M_1}{M_2}\right)^2 \qquad (1)$$

where M_1 and M_2 are the measured collected charges (corrected for polarization effects) at two different polarizing voltages, and the parameters a_j are given in TRS-398. The TVA method was used in **Paper I** to correct for ion recombination in a Baldwin-Farmer type ionization chamber. The method is derived from the function presented by Boag *et al.* (70):

$$\frac{1}{k_s} = \frac{1}{u} \ln\left(1 + u\right) \tag{2}$$

where

$$u = \frac{\mu r d^2}{U} \tag{3}$$

where μ is a constant that depends on the gas in the chamber cavity, r is the initial uniform charge density of positive ions after a brief pulse of radiation, d is the electrode spacing, and U is the polarizing voltage across the chamber. However, this model does not account for the free electrons that are not captured by the polarized oxygen molecules in the chamber cavity and will overestimate k_s at high DPP values (≥ 20 mGy per pulse) (71). To describe volume recombination at high DPP values, Boag *et al.* proposed three models, all including the free-electron fraction, p (59):

$$\frac{1}{k_s'} = \frac{1}{u} \ln\left(1 + \frac{e^{pu}-1}{p}\right) \tag{4}$$

$$\frac{1}{k_s''} = p + \frac{1}{u} \ln\left(1 + (1-p)u\right) \tag{5}$$

and

$$\frac{1}{k_s'''} = \lambda + \frac{1}{u} \ln\left(1 + \frac{e^{\lambda(1-\lambda)u}-1}{\lambda}\right) \tag{6}$$

where

$$\lambda = 1 - \sqrt{1-p} \tag{7}$$

The models described in Eqs. 2, 4, 5 and 6 were used in **Paper I**. However, it has been shown that the Boag theory fails at high polarizing voltages (58,72). As an alternative, Burns and McEwen proposed a semi-empirical model that successfully describes the behaviour of several different ionization chambers at high DPP values (73), but fails at ultra-high DPP values (30). Petersson *et al.* (30) proposed an

empirical logistic function to describe the behavior of the Advanced Markus chamber in these extreme situations:

$$\frac{1}{k_s} = \frac{1}{\left(1+\left(\frac{U[V]}{DPP[mGy]}\right)^{-\alpha}\right)^b}$$ (8)

where α and β are fitting parameters without physical meaning. The authors were then able to use the empirical model to correct for the loss in charge collection efficiency and make the chamber suitable for measurements in UHDR electron beams with an uncertainty of 2.8-4% (30). Eq. 8 was used in **Papers I** and **II** to fit the charge collection efficiency in a transmission chamber as a function of DPP values. More recently, the same model was successfully used to correct for ion recombination in a prototype Razor Nano Chamber (IBA Dosimetry, Schwarzenbruck, Germany) with a smaller sensitive volume than that of the Advances Markus chamber (74). A numerical approach to determine the ion recombination correction based on the charge carrier densities and their transport in the chamber has also been proposed (60).

Radiochromic film

Due to the limitations of ionization chambers in UHDR beams, radiochromic films have been frequently used to determine absorbed dose in radiobiological FLASH studies. In particular, films of the brand Gafchromic (Ashland Advanced Materials, Bridgewater, NJ, USA) have been used. The detection principle is based on the polymerisation of an active layer of diacetylene monomer, which causes a change in colour/optical density when exposed to radiation. The active layer is sandwiched between two layers of polyester for protection. The change in optical density can be related to absorbed dose. The latest generation of Gafchromic films are the EBT3 and EBT-XD models, with a recommended useful dose range of 0.01–20 Gy and 0.04-40 Gy, respectively (75). The dynamic range of the detector is important for the high-dose single fractions that have often been administered in FLASH studies. In **Papers I-V**, radiochromic film (both EBT3 and EBT-XD) have been used for measurements in the UHDR beam.

There are several advantages of radiochromic film, which includes tissue equivalence, energy independence, and high spatial resolution. Importantly, the dose rate independence of the EBT3 and EBT-XD films has been observed up to average dose rates of 1050 Gy/s and pulse dose rates of 10^6 Gy/s in electron beams (28,76,77). Radiochromic film has also been used as a detector in UHDR proton and X-ray deliveries (48,64). However, the major disadvantage of radiochromic film is the time-

consuming read-out, which due to the continued polymerization of the monomer after exposure is typically performed at least 24 h after irradiation.

Other detectors

Semiconductors are a group of charge-based detectors, such as diodes and diamonds, that are generally small and have high sensitivity. Therefore, they often offer a higher spatial resolution compared to gas-filled ionization chambers. In **Paper I**, the response of a clinical *in vivo* diode as a function of DPP was investigated. However, the most promising type of semiconductor for UHDR dosimetry are diamond detectors such as the microDiamond (PTW, Freiburg, Germany), which have shown dose rate independence up to average dose rates of 700 Gy/s in a quasi-continuous 95 keV synchrotron beam (78). However, it should be noted that this source is operated with a PRF of 500 MHz and the pulse dose rate is therefore rather low. In an UHDR electron beam, the response of the microDiamond has been shown to be nonlinear, although Kranzer *et al.* proposed to circumvent this by reducing the sensitive volume and using a low serial resistance of the detector (79). This lead to the development of the protype flashDiamond (80), which was subsequently used for commissioning measurements of a UHDR electron linac (81).

Thermoluminescent dosimeters (TLDs) and alanine dosimeters have been widely used for dose measurements in UHDR beams due to their small size and dose rate independence. In TLDs, impurities are added to create additional energy levels that act as traps for electrons and holes induced by radiation. When exposed to an external stimulus in the form of heat, the trapped electrons and holes can escape, and the resulting luminescent light can be correlated to dose. TLDs have proven to be dose rate independent in electron beams up to average dose rates of at least 1050 Gy/s (76) and pulse dose rates of $4x10^9$ Gy/s (82). In **Paper I** TLDs were used to verify film measurements, and in **Paper III** TLDs were used for dose measurements in an experimental UHDR setup. Alanine is a chemical detector that, after radiation exposure, produces free radicals that are proportional to the absorbed dose. The readout is done with an electron paramagnetic resonance spectrometer. In pulsed beams, alanine is dose rate independent up to pulse dose rates of $3x10^{10}$ Gy/s (83). Unfortunately, both TLD and alanine are passive dosimeters limited to point dose measurements. However, alanine was used for dose verification in the first patient treated with FLASH-RT (24). Gelatin-based polymers are chemical detectors with principles similar to radiochromic film, but with a third dimension. However, gel dosimeters are dose rate dependent (84) and have a complicated readout process.

Aside from ionization chambers (corrected for ion recombination), other detectors suitable for real-time monitoring of machine output and dose delivery in FLASH

beams are scintillation detectors and Cherenkov radiation detectors (64,85,86). Scintillators are tissue-equivalent and independent of energy and dose rate (87–89). The Lynx detector (IBA, Schwarzenbruck, Germany) is a commercially available high-resolution scintillation detector consisting of a gadolinium-based plastic scintillation screen coupled to a CCD camera. This detector has been used in a UHDR electron beam with a stable linear response for pulse dose rates up to 3.5×10^6 Gy/s (85). Cherenkov dosimetry has also proven to be useful in UHDR beams due to the high time resolution and dose rate independence. Cherenkov light is emitted when charged particles travel at a phase velocity that exceeds the phase velocity of light in a certain medium. The Cherenkov signal is proportional to the absorbed dose. Rahman *et al.* showed that the Cherenkov intensity was linear with the dose measured with the EBT-XD film up to average dose rates of 300 Gy/s (90).

Clinical linear accelerator for ultra-high dose rate delivery

The work in this thesis (**Papers I-V**) is centred around an Elekta Precise clinical linear accelerator (Figure 4) that has been modified to allow for a 10 MeV UHDR electron beam. To achieve maximum output, the electron gun filament current is set to a value similar to that used for conventional photon delivery, while the scattering foils and target are retracted. The accelerator is connected to an in-house developed electronic circuit for pulse-to-pulse control. The initial reconfigurations and beam control system have been previously described by Lempart *et al.* (32). Prior to the research presented in this thesis, the beam parameters were further tuned to increase the output, and an upgraded beam control system is currently under development. The radiation delivery is presently managed by a diode that functions as a pulse counter. Once a predetermined number of pulses has been delivered, a signal is transmitted to an optocoupler, which prevents trigger pulses from reaching the thyratron, thereby interrupting the beam. The accelerator can achieve average dose rates of ≥600 Gy/s at the crosshair foil in a setup suitable for cell studies (91,92). For small animal experiments and clinical studies, different electron applicators can be attached to the gantry and fitted with Cerrobend blocks to collimate the field. With this setup, average dose rates of ≥400 Gy/s and ≥180 Gy/s can be delivered at SSDs of 70 cm and 100 cm, respectively. The accelerator can be converted between CONV mode and UHDR mode in just a few minutes, providing a unique platform for conducting studies in a well-known clinical setting. The radiation is delivered in 3.5 μs electron pulses with a PRF of 200 Hz.

Due to the fast delivery, the accelerator's built-in transmission chamber, which is conventionally used for beam monitoring, cannot properly interrupt the beam through the accelerator hardware. In addition, at high DPP values, the charge collection efficiency in the chamber rapidly decreases due to ion recombination effects. This issue is addressed in **Papers I** and **II**. Our long-term goal is to develop a real-time dosimetry system for beam monitoring. In the meantime, other dosimetric methods for accurate UHDR delivery have been established and are presented in **Paper III.** These procedures have allowed for radiobiological studies to be conducted

to compare FLASH and CONV irradiation. Furthermore, to bridge the gap between small animal experiments and clinical trials, a collaboration with veterinarians has been initiated to use FLASH-RT for the treatment of veterinary patients at the accelerator. **Paper IV** presents the establishment and first experiences of these treatments. Finally, **Paper V** examines the potential of intensity-modulated electron FLASH-RT to ensure a homogeneous dose distribution in future clinical veterinary trials.

Figure 4: Photograph of the Elekta Precise linear accelerator modified for ultra-high dose rate delivery, which is used in the work throughout this thesis.

Useful dosimeters

The first step was to investigate which dosimeters could be used in the UHDR beam of the modified clinical linear accelerator. As part of **Paper I**, the dose rate dependence of TLDs, a Baldwin-Farmer type chamber, and an EDP 20-3G *in vivo* diode was investigated by measuring their response with increasing DPP values. The

DPP values were controlled by adjusting the electron gun filament current. EBT3 film was used as the primary dosimeter to measure the DPP for each exposure. All dosimeters were irradiated simultaneously to remove uncertainties associated with output variations. The film was positioned at a reference position at a depth of 2 cm in a 10 cm thick slab of solid water positioned at an SSD of 100 cm. The films were scanned 24 hours after exposure using a flatbed scanner and analyzed in Image J. The DPP values ranged from 0.6 mGy per pulse to 0.99 Gy per pulse, corresponding to average dose rates from 0.1 Gy/s to 198 Gy/s. The TLD was positioned just below the EBT3 film, the ionization chamber was positioned in the bremsstrahlung tail of the depth dose curve (at a depth of 9 cm in the phantom), and the diode was positioned at the top of the phantom close to the beam edge.

The results showed that there was a linear relationship between the TLD and the EBT3 film in the measured DPP range. Assuming a dose rate independence of EBT3 film (77), these findings confirmed previous results demonstrating the dose rate independence of TLDs (82). The response of the Baldwin-Farmer ionization chamber was corrected for recombination effects using the TVA method (Eq. 1) and for polarity effects. The results indicated that the chamber response was linear with the DPP measured with the EBT3 film up to approximately 0.7 Gy per pulse (corresponding to an average dose rate of approximately 4 Gy/s at the chamber position), after which a plateau was reached. This suggested that even though the chamber was placed at a depth of 9 cm in the phantom, the TVA method was insufficient to correct for ion recombination at the highest dose rates achievable with the modified clinical linear accelerator. The response of the diode saturated above approximately 0.4 Gy per pulse as measured by the EBT3 film.

Based on these findings, it was concluded that EBT3 film and TLDs are suitable detectors for use in the UHDR electron beam of the modified clinical linear accelerator. However, the diode was found to be unsuitable, and the Baldwin-Farmer type ionization chamber was of limited use, for dose measurements in the UHDR beam. Although the Baldwin-Farmer type ionization chamber was impractical and imprecise for use at dose rates exceeding 4 Gy/s, it might still be useful for relative output measurements, as demonstrated in **Papers III and IV**.

Reference dosimetry

As previously noted, there is currently no international code of practice for reference dosimetry under UHDR conditions. The UHDpulse workgroup is working intensely to establish the necessary metrological tools to achieve traceability in absorbed dose

measurements for particle beams with ultra-high DPP values (56). For reference dosimetry in clinical high-energy electron beams (3-50 MeV), the recommended method is to use plane-parallel chambers that are calibrated in an electron beam, either directly at a standards laboratory or by cross-calibration in a clinical electron beam (57). The chambers should be corrected for ion recombination effects with the TVA method (57). However, the TVA method fails at high DPP values (93).

Since the UHDR source at our department is a medical linear accelerator, reference dosimetry could be performed in the clinical 10 MeV beam in accordance with the IAEA TRS 398 Code of Practice (57). Thus, the absorbed dose to water in the clinical 10 MeV beam, $D_{w,Q}$, was determined using a plane-parallel Roos electron chamber (type 31004, PTW Frielburg, Germany) traceable to a standards laboratory as (Figure 5, left panel):

$$D_{w,Q} = M_Q N_{D,w,Q_0} k_{Q,Q_0} \qquad (9)$$

where M_Q is the ionization chamber reading corrected for influencing quantities, N_{D,w,Q_0} is the calibration coefficient in terms of absorbed dose to water for the reference beam quality Q_0, k_{Q,Q_0} is the chamber specific correction factor for the difference in the ionization chamber response between Q and Q_0.
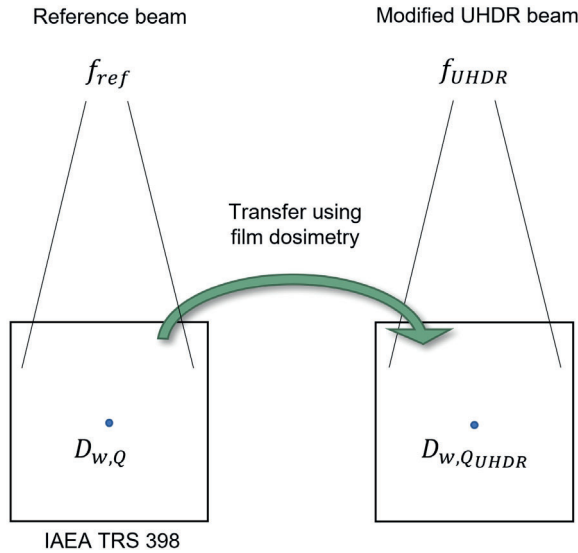
Figure 5: Methodology for reference dosimetry in the electron beam used for ultra-high dose rate (UHDR) delivery using the modified clinical linear accelerator.

To determine the absorbed dose to water at the reference depth in the modified field at UHDR conditions, $D_{w,Q_{UHDR}}$, we applied a field output factor $\Omega_{Q,Q_{UHDR}}$ according to (Figure 5, right panel):

$$D_{w,Q_{UHDR}} = D_{w,Q}\Omega_{Q,Q_{UHDR}} \qquad (10)$$

The field output factor was measured using radiochromic film. Both GafChromic EBT3 and EBT-XD films were calibrated in the clinical 10 MeV beam in a Solid Water HE phantom (Gammex Inc., Middleton, Wisconsin, USA) for a dose range 0-30 Gy (0-40 Gy for EBT-XD). Films were handled, processed, and analyzed according to the guidelines provided in the AAPM Task Group 235 report (75). The absorbed dose measured with film at UHDR conditions have also been verified with alanine measurements.

Beam monitoring

For a successful clinical implementation of UHDR radiotherapy, a redundant dosimetry system with high temporal resolution for real-time dose monitoring of the beam is of outmost importance. Traditionally, transmission chambers are used to monitor and interrupt the beam when the desired dose has been delivered. The transmission chamber is a large plane-parallel ionization chamber consisting of two dose plates and one servo plate. It is designed to monitor delivered dose and dose rate, and to report information about beam flatness and symmetry. This system is part of every clinical linear accelerator and is permanently mounted in the beam path in the gantry head. The collected charge in the two dose channels is quantified in terms of monitor units (MU) and calibrated against an ionization chamber traceable to a standards laboratory. However, when the accelerator is operated in FLASH mode, the transmission chamber cannot currently be used to monitor the beam due to severe ion recombination effects. In the previous chapter it was presented as a possible solution to increase the charge collection efficiency in ionization chambers by reducing the electrode spacing and increasing the polarizing voltage. Such an approach could potentially make transmission chambers useful in UHDR beams. In **Paper I**, the behaviour of the built-in transmission chamber of the clinical linear accelerator at elevated DPP values was explored. In addition, the polarizing voltage was increased by a factor of 2 or 3 to increase the collection efficiency of the chamber. A logistic function was fitted to the data points and used to correct for the remaining loss in efficacy due to ion recombination. **Paper II** examined the potential of reconfiguring the design and operation of a transmission chamber to further increase the charge

collection efficiency. In **Paper II**, an external transmission chamber was attached to the electron applicator, the electrode distance was reduced, and the polarizing voltage was increased.

## Ion recombination in a built-in transmission chamber

As a first step in investigating the potential of using a transmission chamber for real-time dosimetry and beam monitoring of UHDR beams in a clinical setting, the built-in transmission chamber of the clinical linear accelerator was used (**Paper I**). The raw signal from one of the dose channels with an electrode spacing of 1 mm and a standard (negative) polarizing voltage of 320 V was extracted from the linac to study the chamber behaviour with increasing DPP. The response of the chamber was extracted simultaneously with the response of the TLD, Baldwin-Farmer type chamber, diode, and EBT3 film in the setup previously described. Since the film could not be placed at the chamber position inside the gantry head, the DPP was determined at 2 cm depth in the phantom.

The set of influence quantities described in IAEA TRS 398 (57) was used to relate the collected charge per pulse in the built-in transmission chamber to the DPP in the solid water phantom. Assuming that the temperature, humidity, and electrometer response did not change with varied DPP value, and that the recombination correction factor is unity for CONV irradiation, the charge collection efficiency in the transmission chamber for a certain dose rate could be calculated as the ratio between the collected charge per unit dose and the collected charge per unit dose at CONV irradiation. Note that in **Paper I** the term ion collection efficiency is used instead of charge collection efficiency.

In **Paper I**, a rapid drop in charge collection efficiency was observed under standard operation of the transmission chamber (320 V) when exceeding DPP values of approximately 10^{-3} Gy per pulse (average dose rates of ~20 Gy/min). At the highest achievable DPP value, i.e., the level used for UHDR irradiations, the charge collection efficiency was only 10%. The measurements were repeated with the chamber voltage increased by a factor of 2 and 3 (i.e., 640 V and 960 V). Figure 6 presents the chamber signal per pulse as a function of DPP for chamber voltages of 320 V, 640 V and 960 V, respectively, and show that the relation is non-linear for all three voltages. However, by increasing the chamber voltage the charge collection efficiency at the highest achievable DPP value could be increased to 14% and 22% for 640 V and 960 V, respectively. The DPP operating range of the chamber, i.e., the range of DPP values requiring no or minor corrections for the recombination effect,

was extended to approximately 4×10^{-2} Gy per pulse at 960 V, which corresponds to an average dose rate of ~10 Gy/s at the reference position.

In **Paper I**, an empirical model was used to describe the drop in charge collection efficiency by fitting the logistic function suggested by Petersson *et al.* for the Advanced Markus chamber (Eq. 8) to the measured data. Since the DPP was determined at the reference position and not in the chamber, a factor of 10 had to be multiplied into the model to ensure a good agreement between the data points and the model. The four Boag models (Eqs. 2, 4, 5 and 6) were also fitted to the data points, with a good agreement only at 320 V. For higher polarizing voltages, Boag's functions overestimated the charge collection efficiency at high DPP values. This is consistent with the findings of previous reports (30,58,60).
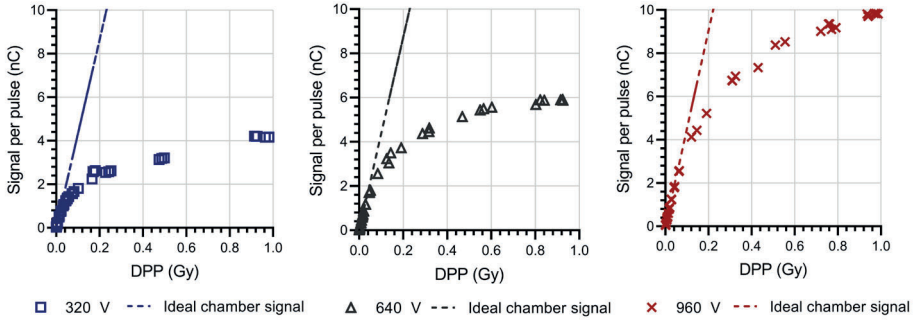

Figure 6: Chamber signal per pulse as a function of dose-per-pulse (DPP) values for operating negative polarizing voltages of 320 V (left), 640 V (center), and 960 V (right), for the built-in transmission chamber. The ideal chamber signal is represented as dashed lines.

To enable practical determination of the ion recombination correction factor from the transmission chamber signal when the DPP is unknown, the empirical model was reformulated to be a function of the apparent DPP. Also, for this version of the model, a good agreement was found between the data points and the model. However, the slope of the charge collection efficiency curve was steep at the DPP values associated with UHDR delivery, increasing the uncertainty in the recombination correction factor compared to the flat slope present at CONV DPP values. Therefore, it would be beneficial to further increase the charge collection efficiency and to operate the chamber in a region where the charge collection efficiency curve is flat. Considering that the linac was also used in clinical mode, the

chamber voltage was not increased above 960 V in **Paper I** due to the risk of damaging the built-in transmission chamber and surrounding components in the gantry head.

Reconfiguring an external transmission chamber

In **Paper II**, the potential to further decrease the general recombination was investigated in two transmission chambers of the same type as the built-in chamber, mounted one-by-one in the upper part of the electron applicator (Figure 7). In this position, the transmission chambers were exposed to approximately 3 Gy per pulse, which is considerably less than at the position of the built-in transmission chamber and should mitigate the effect of ion recombination. Additionally, this experimental setting allowed for chamber modifications without compromising the clinical use of the linac. One of the transmission chambers was reconfigured by reducing the electrode distance from 1 mm to 0.6 mm. The goal was to extend the range of DPP values with no or minimal recombination effects up to the UHDR regimen, i.e., corresponding to an average dose rate ≥40 Gy/s in the treatment position.
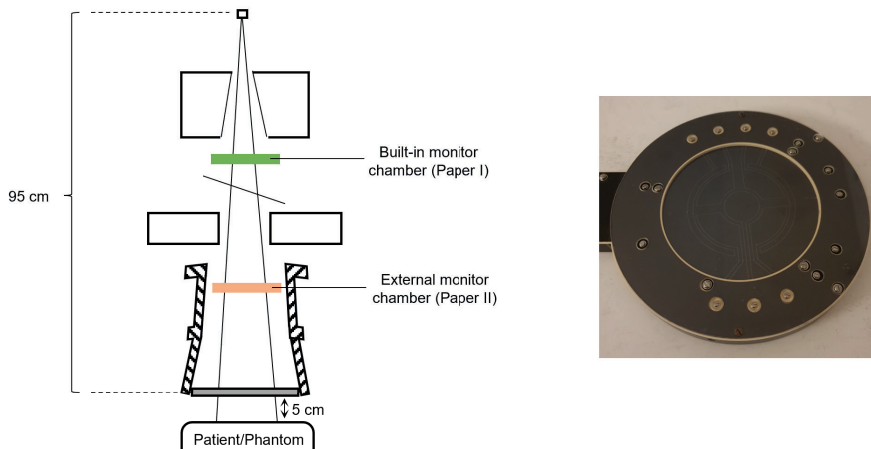
**Figure 7:** Left: Setup used for measurements with an external transmission chamber, mounted in the upper part of the electron applicator at the clinical linear accelerator. Right: Photograph of the type of transmission chamber used in Paper I and II.

As in **Paper I**, the DPP values in **Paper II** were controlled by adjusting the electron gun filament current. The DPP values in the treatment position (2.2 cm depth in the

10 cm solid water slab), $DPP_{phantom}$, ranged from 0.58 mGy per pulse to 0.86 Gy per pulse, corresponding to average dose rates from 0.12 Gy/s to 170 Gy/s. Compared to **Paper I**, the DPP values in **Paper II** could also be estimated at the position of the chamber, $DPP_{chamber}$, by applying a proportionality factor obtained from relative film measurements at the treatment position and at the position of the transmission chamber. $DPP_{chamber}$ ranged from 2.3 mGy per pulse to 3.4 Gy per pulse, corresponding to average dose rates from 0.46 Gy/s to 680 Gy/s. The signal of both transmission chambers was measured as a function of DPP, and the charge collection efficiency was determined at each data point.

In the first set of measurements, the transmission chamber signal per pulse was measured as a function of $DPP_{phantom}$ for the chamber with a 1 mm electrode spacing operated at 320 V. To determine the effect of reducing the dose rate at the transmission chamber position while maintaining a similar dose rate at the treatment position, these measurements were compared to the signal of the built-in transmission chamber in **Paper I** operated under the same conditions. The results showed that the chamber signal was non-linear with $DPP_{phantom}$ for both setups. For the external transmission chamber in **Paper II**, the charge collection efficiency at the highest achievable DPP was 24%, compared to 10% for the built-in transmission chamber in **Paper I**.
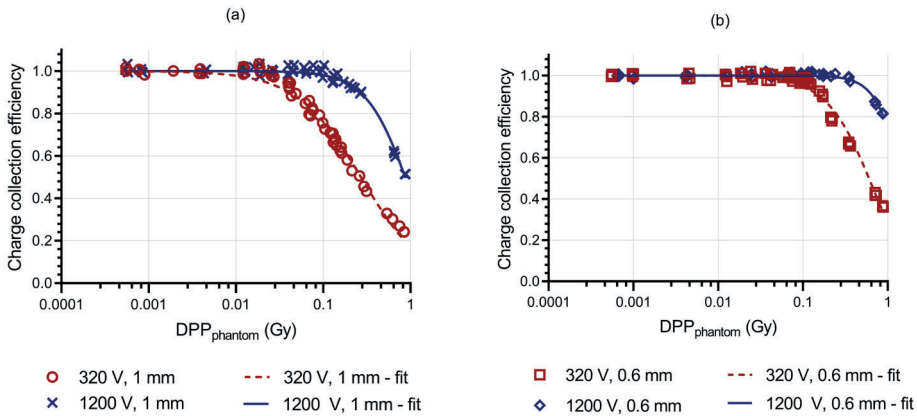
Figure 8. Charge collection efficiency of the transmission chamber as a function of $DPP_{phantom}$ for the chamber with (a) 1 mm and (b) 0.6 mm electrode spacing, for chamber voltage of 320 V and 1200 V, as well as the logistic fit (Eq. 11). Figure from paper II.

In **Paper II**, the measurements were repeated for the transmission chamber with a 0.6 mm electrode distance to investigate the effect of reducing the electrode distance of the chamber. This resulted in a charge collection efficiency at the highest achievable DPP of 36%, i.e., an increase in charge collection efficiency by a factor of 1.5 compared to the transmission chamber with 1 mm electrode distance (Figure 8).
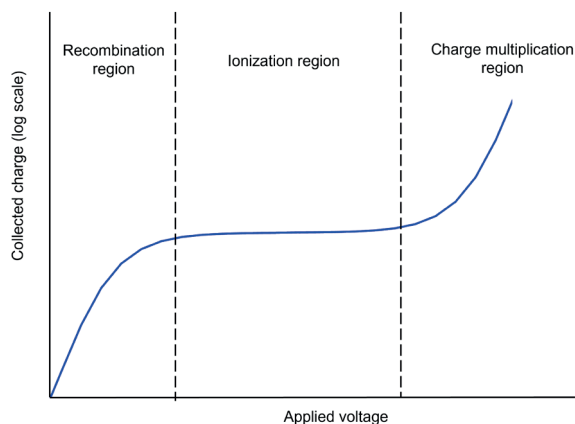
Figure 9: Illustration of a typical charge-voltage curve. In the recombination region, many collected ion pairs recombine before reaching the cathode. In the ionization region, the field strength is adequate to collect all produced ions. In the charge multiplication region, the electrons have enough energy to cause additional ionizations in the chamber air volume.

The effect of adjusting the chamber voltage was investigated in more detail in **Paper II** compared to **Paper I**. A typical behaviour of ionization chambers as a function of the applied voltage is illustrated in Figure 9. At CONV irradiation, the transmission chamber with 1 mm electrode distance showed a stable response between 200 V and 1500 V, but in the transmission chamber with 0.6 mm electrode distance the response increased drastically above 1300 V, indicating the presence of charge multiplication in this chamber at this voltage level. At UHDR, the transmission chambers operated in the recombination region, with an increased response with increased voltage. This behaviour is in line with recent results by Kranzer *et al.*, which showed an increased steepness of the current-voltage curve with increased DPP (65). In **Paper II**, the highest possible safe voltage level was found to be 1200 V. This voltage was chosen for further investigation of the response and charge collection efficiency as a function of DPP, to achieve the maximum charge collection efficiency but avoiding charge multiplication. Our results did not show any difference in the

calibration coefficient (collected charge per unit dose at CONV) between 320 V and 1200 V, also indicating that there was no effect of charge multiplication at these voltage levels. For a chamber voltage of 1200 V, the charge collection efficiency at the highest achievable DPP was 51% and 82% for the transmission chambers with electrode distances of 1 mm and 0.6 mm, respectively (Figure 8). Thus, for all four investigated combinations of electrode distance and chamber voltage, the chamber signal was linear only for a limited range (Figure 10).
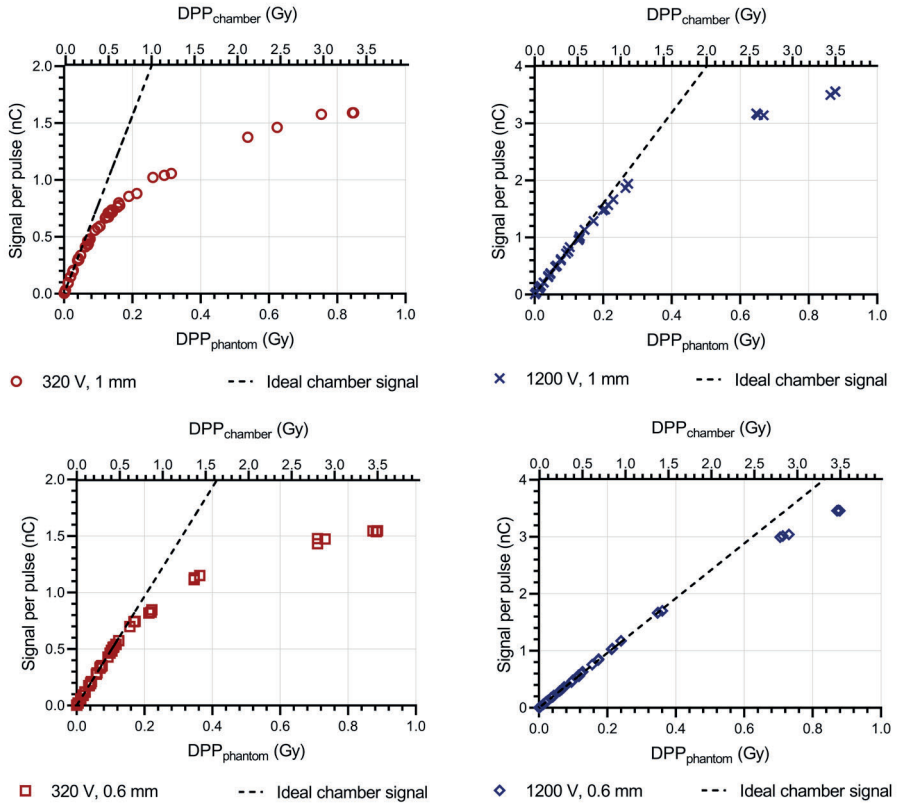
Figure 10: Chamber signal per pulse as a function of $DPP_{phantom}$ (lower axis) and $DPP_{chamber}$ (upper axis) for the two different chambers with 1 mm (upper panel) and 0.6 mm (lower panel) electrode distance, respectively, and for two different negative chamber voltages of 320 V (left panel) and 1200 V (right panel). The ideal chamber signal is represented as dashed lines. Figure from paper II.

A logistic function similar to the one proposed by Petersson *et al* (Eq. 8) but with the electrode distance, d, incorporated, was used to fit the data points:

$$CCE = \frac{1}{\left(1+\left(\frac{DPP_{chamber} * d^2}{U}\right)^\alpha\right)^b} \qquad (11)$$

where $DPP_{chamber}$ is given in mGy, d is the electrode distance in mm, U is the chamber voltage in V, and α and β are fitting parameters. The agreement between the data points and the model was good (Figure 8), suggesting that this function can successfully describe the behaviour of the chamber at ultra-high DPP values. For the transmission chamber with 0.6 mm electrode spacing operated at 1200 V, the charge collection efficiency was constant up to $DPP_{phantom}$ of 0.35 Gy, corresponding to an average dose rate of 70 Gy/s at the treatment position at SSD=100 cm.

Discussion

The aim of **Papers I** and **II** was to decrease the general recombination in a transmission chamber to make it useful for real-time dosimetry and beam monitoring in an UHDR electron beam. Correction for ion recombination in ionization chambers in UHDR beams have been investigated in several other studies (30,60,65,74). However, the behaviour of the built-in transmission chamber has not previously been investigated under these conditions. When utilizing already existing clinical linear accelerators for UHDR irradiation, it would be convenient if the transmission chamber could still be used as a beam monitor and control system.

In **Paper I**, it was found that the charge collection efficiency of the built-in transmission chamber operated at the standard voltage (-320 V) was 10% at the highest achievable DPP, and that by increasing the polarizing voltage by a factor of 3 the charge collection efficiency was increased to 22%. In **Paper II**, an external transmission chamber was positioned downstream in the beams path, and by reducing the electrode distance to 0.6 mm and use the maximum safe voltage of 1200 V the operating DPP range of the transmission chamber was extended up to the UHDR regimen of several Gy per pulse. This allowed for full charge collection efficiency up to an average dose rate of 70 Gy/s in a clinical treatment position, and >82% charge collection efficiency up to 180 Gy/s. **Papers I** and **II** also demonstrated the successful fitting of the charge collection efficiency using a logistic function incorporating the chamber voltage (and the electrode distance in **Paper II**).

In **Papers I** and **II**, we used radiochromic film as the primary detector to measure the delivered DPP. The radiochromic film has an intrinsic uncertainty which is greater

than that for ionization chambers. Therefore, this method for real-time output measurements does not allow for uncertainties below that of film measurements. One option for a more accurate model is to use alanine pellets, which are more widely accepted for absorbed dose measurements and has been shown to be dose rate independent up to 10^{10} Gy/s (94). Another option suggested by McManus *et al.* is to measure the charge collection efficiency in the chamber against a primary standard graphite calorimeter (95).

The ionization chambers should preferably be operated in the ionization region of the charge-voltage curve to enable all created ion pairs to be collected. However, in **Paper II** it was found that for the highest DPP value achievable by the electron beam from the modified clinical linear accelerator, no such region exists. The transmission chamber can still be operated under these extreme conditions, but it is important to make sure that the chamber do not enter the charge multiplication region, where the generated electrons have enough energy to cause additional ionization in the air of the chamber, causing a cascade effect. In **Paper II**, the highest possible safe voltage level was chosen to achieve maximum charge collection efficiency but avoiding charge multiplication.

There are still potential adjustments that can be made to further increase the range of DPP values with no or minor recombination effects. One alternative is to further reduce the electrode distance. However, this requires careful investigation to ensure that the charge multiplication region is not reached. Gomez *et al.* showed that the charge multiplication region was observed already >250 V for a small plane-parallel ionization chamber with an electrode distance of 0.22 mm (66). In addition, such small gaps are challenging to construct. Another option, as suggested by Di Martino *et al.*, is to change the gas inside the chamber (68). However, this would require a sealed chamber.

Another recently explored option for beam monitoring is the use of beam current transformers (BCTs) (96–98). Commercially available BCTs have been successfully implemented at the exit of the preclinical Oriatron eRT6 linac, and at the exit of the clinical Mobetron (96,97). More recently, a dual BCT design was integrated into the head of the Mobetron also to allow for the beam energy to be determined (98). BCTs consist of a toroid sensor, an external electronic system, and a power supply and are already widely used in high-energy physics. The induced current is measured and provides a live temporal readout of the total exit charge. It has been shown that the exit charge is proportional to the absorbed dose and that long-and short-term stability is acceptable (96,97). However, in contrast to traditional transmission monitor chambers, the BCTs cannot be used to obtain information about beam parameters

such as flatness and symmetry. In addition, the capability of this approach to control and interrupt the beam has yet to be investigated.

Future perspectives

Before FLASH-RT is ready for large-scale clinical implementation, one of the technical challenges is to develop a stable beam control system that can deliver any prescribed dose at high DPP values. In the current setup, the interruption of the UHDR beam of the modified clinical linear accelerator depends solely on a pulse-counting diode placed in the radiation field. Ideally, the two dosimetry channels of the transmission chamber can be independently used to interrupt the beam, which would increase safety during UHDR delivery with an approach similar to the method used to control the delivery in CONV-RT. Additionally, to allow robust radiobiological studies that can be compared regarding the time structure, it is essential to control and receive real-time feedback on the delivered dose, the number of pulses, PRF, and delivery time. The beam control system used to control and interrupt the UHDR beam of the clinical linear accelerator is currently being further developed to meet these criteria.

The new system will control the UHDR beam based on the charge collected by the transmission chamber mounted in the electron applicator and corrected according to the correction strategy developed in **Papers I** and **II**. The system will primarily interrupt the beam based on dose. The operator can set the desired amount of monitor units to be delivered. For increased safety, the beam can also be interrupted based on a set number of electron pulses counted by the pulse counter. In case of failure of both the transmission chamber and the pulse counter, the equipment will be designed to also interrupt the irradiation based on time since the start of the irradiation. The system consists of three in-house built circuit boards. It displays information about the delivered dose, number of pulses, time from the beam-on to the end of the last pulse, and estimated PRF following each delivery. In future work, the system will be validated in terms of accuracy and long- and short-term stability.

The new system will include a feature to adjust the dose in the first pulse, which may address the current limitation of only being able to deliver doses that are a multiple of the DPP. This will be achieved by monitoring the uploading cycle of the pulse forming network (PFN) charge and setting a time delay to control when the thyratron trigger pulses are released to the accelerator. Preliminary work has shown that without a time delay, the trigger pulses will not be in sync with the PFN upload, resulting in a low output in the first pulse. After the first pulse, the PFN and the thyratron trigger

pulses are in sync with a full upload of the PFN (and thus maximum output) for the remaining pulses. This way, the output in the first pulse can be varied by varying the PFN time delay. A more sophisticated method of fine-tuning the delivered dose would be to adjust the dose in the last pulse based on what has been delivered in the previous pulses. This will also be explored in future work.

Translational research in FLASH radiotherapy

Dosimetric procedures for experimental irradiations

While the development of a real-time dosimetry system for beam monitoring at UHDR is ongoing, radiobiological studies are conducted at the modified clinical linear accelerator. For reliable and reproducible radiobiological experiments, it is crucial with robust dosimetry procedures. To ensure this, experimental setups and dosimetric procedure for preclinical studies at UHDR were established in **Paper III.** To investigate the difference between CONV-RT and FLASH-RT *in vitro*, several cell studies have been performed at the modified clinical linear accelerator (91,92). In these experiments, the gantry was set to 180 degrees and T12.5 cell flasks containing cells and cell media were placed one-by-one on top of the gantry cross-hair foil (**Paper III**). The pulse counter was placed in the radiation field next to the cell flask to enable interruption of the beam after a pre-set number of pulses. The field size for this setup was measured with EBT3 film at the cross-hair foil. In the area covered by the cell flask the beam flatness was 2.2%. DPP was determined before and after each set of irradiations by placing the EBT3 film at the bottom of a cell flask under a 2 mm sheet of polystyrene mimicking cell media. In addition, the Baldwin-Farmer type ionization chamber was attached to the ceiling of the room within the radiation field and used for relative output measurements to ensure stable dose delivery throughout the cell irradiations.

The sparing effect of FLASH-RT compared to CONV-RT has also been studied in zebrafish embryos, at the Elekta Precise (unpublished work) and elsewhere (18,64,99). For irradiation of zebrafish embryos, a similar setup as for cell experiments were used, but with the embryos collected in Eppendorf tubes instead of flasks (**Paper III**). The Eppendorf tubes were fitted one-by-one into a 3D printed plastic phantom (Figure 11, left panel). In the area covered by the 3D printed phantom the beam flatness was 2.7%. To enable TLD dose measurements, a 3D printed insert in the shape of an Eppendorf tube with empty slots for TLDs was

designed (Figure 11, right panel) and fitted into the 3D printed phantom. In addition, a similar 3D printed phantom was constructed for film measurements. The DPP for this setup was determined by TLD and film measurements before and after each zebrafish embryo irradiation.
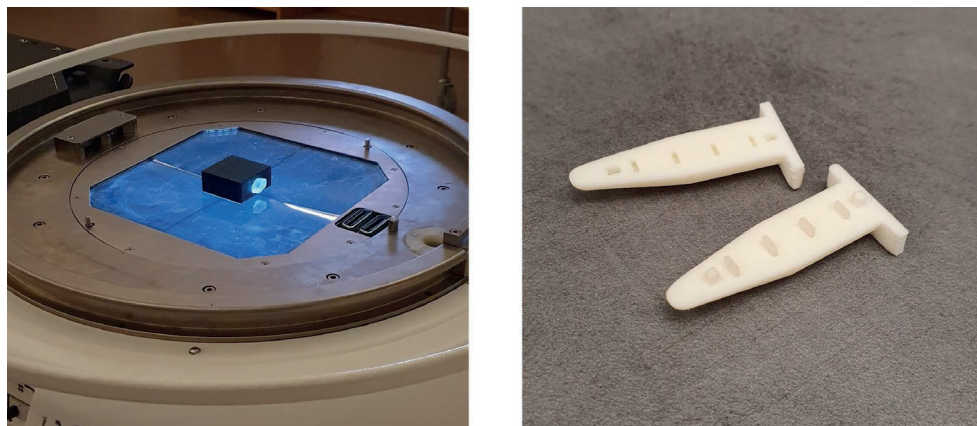
Figure 11: Left: The setup used for irradiation of zebrafish embryos at the modified clinical linear accelerator. Embryos were collected in a Eppendorf tube and fitted in a 3D printed plastic phantom. Right: A 3D printed insert in the shape of an Eppendorf tube, with slots for TLDs.

The clinical linear accelerator has also been used to study the anti-tumour effect of FLASH-RT compared to CONV-RT in an immunocompetent rat glioma model (100,101). In addition, the sparing effect of FLASH-RT has been investigated in a mouse melanoma model (submitted). For these irradiations, a short electron applicator was used (source-to-applicator-end distance of 65 cm), fitted with Cerrobend blocks with different cut-outs to collimate the field. The animals were placed in plastic boxes in direct contact with the Cerrobend blocks. In **Paper III**, dose profiles, depth dose curves, and output factors were determined for each available field size using EBT-XD film. DPP values were determined by film measurements at the same depth as the tumour (or skin) in plastic phantoms placed inside the plastic boxes, both before and after the animal irradiations. For some experiments, the Baldwin-Farmer type ionization chamber was placed in a solid water phantom under the box and used for relative output measurements during the irradiation. Additionally, when feasible, EBT-XD film was used for *in vivo* measurements during irradiations.

FLASH radiotherapy in larger animals

In vitro and *in vivo* models can guide the selection of conditions and beam parameters to be tested in clinical trials. However, there is a translational gap between the laboratory setting and human clinical trials (Figure 12), and generally many preclinical findings fail in clinical translation (102). A possible solution to obtain controlled evidence on the potential benefits and limitations of FLASH-RT is to conduct studies involving larger animals. In 2019, Vozenin *et al.* reported irradiation of a minipig in which single doses of 22-34 Gy were administered to multiple circular patches of the skin with FLASH (~300 Gy/s) or CONV (~5 Gy/min) electron irradiation (21). Severe toxicities related to depilation, fibronecrosis, epithelial ulceration, and inflammation were observed in areas irradiated with CONV. On the contrary, FLASH-irradiated skin resulted in only minor depilation and pigmentation. The authors suggested a dose-protective factor of at least 20% for FLASH-RT. In the same publication, the treatment effect was evaluated in a phase I dose-escalation trial involving six feline cancer patients with advanced squamous cell carcinoma (SCC) of the nasal planum (21). Although no CONV group was included for comparison, the results were encouraging. Treatments were administered in a single fraction at prescribed doses ranging from 25 Gy to 41 Gy. At 6 months, all cats were in complete remission and at 18 months 3/6 cats were disease-free. Acute toxicities consisted of no or mild dermatitis/mucositis, and no late-stage toxicities other than depilation were reported during the median follow-up of 18 months.

Indeed, companion animals could serve as a valuable tool to bridge the gap between laboratory research and clinical applications. They develop spontaneous cancers of sizes and types that parallel those of humans and can therefore be treated with similar field sizes and energies. This is a great advantage for the clinical translation of new radiotherapy techniques. Additionally, companion animals are immunocompetent and are exposed to the same environment and toxic substances as humans. Translational research with companion animals offers a potential win-win situation, where the veterinary patients may benefit from advanced diagnostics or treatments that are otherwise not available to them, while also providing information that can help optimize future human clinical trials.

A veterinary clinical trial in canines with extremity osteosarcoma was recently reported from the University of Pennsylvania (23). The dogs were treated with a single fraction of a standard proton beam or with a FLASH proton beam at 8 or 12 Gy, and after 5 days the limb was amputated. The main objective of the study was to evaluate the effects of treatment by studying biopsies from the amputated limb. For limbs irradiated with 12 Gy, the ratio of TGFβ1 expression (an agent of radiation-

induced inflammatory reactions) in irradiated versus unirradiated tissue of the same animal was higher in patients treated with the standard proton beam compared to the FLASH proton beam, suggesting a protective effect of FLASH in this clinical setting.
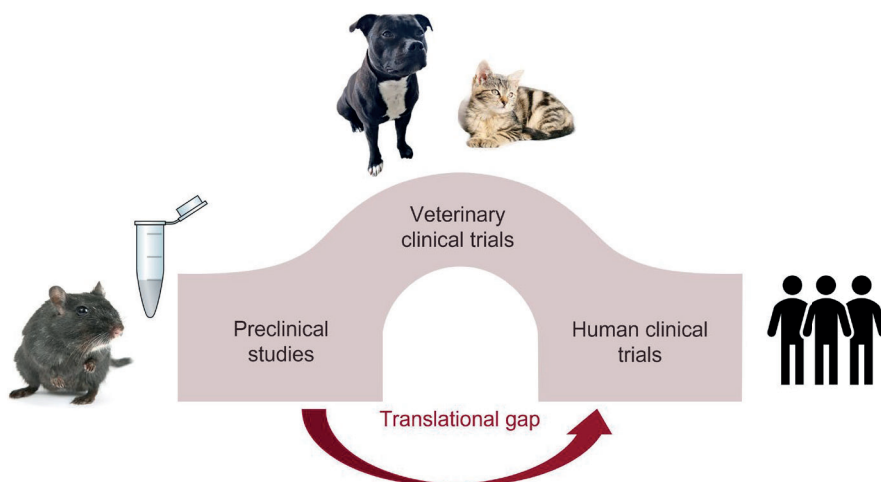
Figure 12: Veterinary clinical studies can help bridge the translational gap between the laboratory setting and human clinical trials.

Clinical establishment and experience in canine cancer patients

As a step towards human clinical trials at the clinical linear accelerator described in this thesis, a collaboration with veterinarians at the University of Copenhagen was initiated. Within this collaboration, 28 canine and 3 feline cancer patients have been treated with FLASH-RT. The patients either had no other relevant treatment option or the owners had decided against standard therapy. Also, to be included in the study, the treating veterinarian had to believe that the patient would benefit from FLASH-RT. It should be noted that CONV-RT is not available for veterinary patients in Denmark. The aim of the collaboration is to explore FLASH-RT in a clinically relevant setting and to establish procedures for future human clinical trials.

Setup and workflow

In **Paper IV**, dosimetric procedures and a clinical workflow for the treatment of companion animals with FLASH-RT were established on the modified clinical linear accelerator. Patients were treated with a 5 cm gap from the distal edge of an electron applicator with a source-to-applicator-end distance of 65 cm, i.e., at an SSD of 70 cm (Figure 13, left). To shape the beam close to the targets, Cerrobend blocks with cut-outs of different geometries and field sizes were custom-made. The beam was characterized by EBT-XD measurements of dose profiles and percentage depth dose curves. The information was used together with clinical examination, calliper measurements, and CT images and/or photographs of the tumour to plan the treatments in terms of bolus and field size.

The built-in transmission chamber was not used to monitor the beam due to the issue of ion recombination. Instead, EBT-XD measurements were performed prior to each treatment in phantoms mimicking the treatment geometry, to determine the DPP at dose maximum for the given patient and the number of pulses to be delivered to reach the prescribed dose. To ensure that the prescribed dose was delivered during the actual treatment, the Baldwin-Farmer type ion chamber was used for relative output measurements and EBT-XD film was used for *in vivo* dose measurements at the skin surface to verify the delivered dose.

Figure 13: Two examples of treatment setups for FLASH radiotherapy of canine cancer patients at the modified clinical linear accelerator.

In some of the canine patients, the tumours were growing in the palate and the treatments were administered through cylindrical PMMA applicators aligned perpendicular to the collimator using soft docking (103) (Figure 13, right). Film measurements during treatment were then performed in the collimator block cut-out and related to the dose delivered at the dose maximum via phantom measurements. These intracavitary treatments were not included in the setup description in **Paper IV** but are reported elsewhere (104,105).

Initial experience

The initial experience of the first 10 canine cancer patient treatments was reported in **Paper IV**, including feasibility and safety, treatment parameters, possible adverse events, and treatment response. The patient group was heterogeneous and included seven patients with solid superficial or subcutaneous tumours of different types, and three patients with post-operative microscopic disease. The trial was designed as a dose-escalation trial and the chosen treatment parameters were based on previous experimental treatments (21,24) starting at an absorbed dose of 15 Gy in a single fraction (Figure 14). All tumours received a single beam single fraction of FLASH-RT, except for one tumour, which was irradiated with a second dose one month after the first treatment.
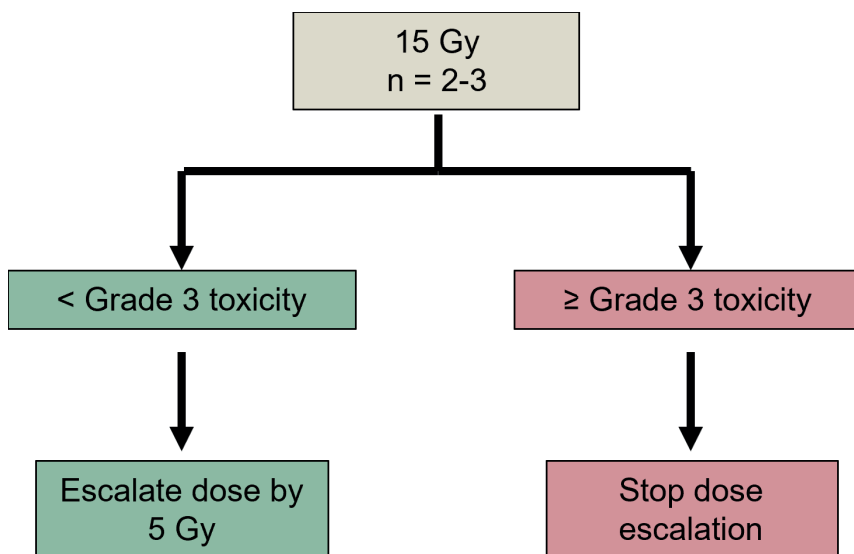
Figure 14: Design of the dose-escalation trial part of Paper IV.

Based on the *in vivo* film measurements, the dose was accurately delivered with an average agreement with the prescribed dose of 1.8% (range -9.4 % to +5 %). In **Paper IV,** it was found that 11/13 irradiated tumours either had partial response, complete response or stable disease following treatment. Adverse events observed at follow-up (ranging from 3-6 months) were generally mild and consisted of local alopecia, leukotricia, dry desquamation, mild erythema, or swelling. A grade 3 skin adverse event was observed in a patient receiving 35 Gy at maximum dose with the sensitive nasal planum included in the treatment field. However, this patient was in complete clinical remission at the 1- and 3-months follow-up.

The next step was to use this experience as the basis for a phase-II veterinary single-arm trial with a more specific patient inclusion selection. In this study, eleven canine patients with oral malignant tumours were included (105). The primary endpoint was to evaluate the feasibility and safety of using single-fraction FLASH-RT to treat malignant tumours of the oral cavity. Treatment efficacy was evaluated as a secondary endpoint. Patients received a single fraction FLASH-RT with prescribed dose to the depth of dose maximum ranging between 30-42 Gy, depending on the tumour status and size. The patients were followed for 12 months, with imaging performed at 6 and 12 months if bone was included in the radiation field. It was found that the treatment had a good clinical efficacy, with an overall response rate of 100%, and for most cases with complete remission the effect was durable long-term. However, it was also found that there was a high risk of adverse events if bone was included in the treatment field. At the 12-month follow-up, three of the four surviving dogs had developed osteoradionecrosis. It was concluded that long-term follow-up is needed for each organ/tissue before a safe clinical translation of FLASH-RT (105). A reconstruction of the dose distribution was created for one of the oral patients that developed bone necrosis. The patient was treated with an open mouth using a PMMA applicator to reach the tumour located in the hard palate. The bone necrosis was developed at a location with reduced bone density prior to the treatment. The dose reconstruction demonstrated a maximum dose outside the target of 120% (42 Gy) in the heterogeneous region of bone and air, with the bone area where the osteoradionecrosis was developed receiving up to 114% (40 Gy).

As previously described, some of the oral treatments were performed with a PMMA tube as an applicator. This method is similar to intraoperative radiotherapy (IORT), where the radiotherapy is carried out during surgery with an applicator positioned directly over the tumour. For the first patient treated with intracavitary FLASH-RT using a PMMA applicator at the Elekta Precise, the feasibility was demonstrated by presenting the dosimetric procedure, side effects and treatment response (104).

Discussion

Paper IV describes the first experience of electron FLASH-RT in a clinical setting. Previous FLASH-RT treatments had been conducted at industrial-type electron accelerators (21,24). The treatment results were promising, with only mild short-term toxicity in all included patients except for one patient for which the sensitive part of the nose was included in the treatment field, causing a grade 3 adverse effect. Due to the heterogeneous group of patients recruited for FLASH-RT at the clinical linear accelerator, **Paper IV** was not designed to provide any statistical evidence of the benefit of FLASH-RT compared to other treatment protocols, which clearly is a limitation of the study. The same goes for the later cohort including canine patients with oral tumours. However, these studies have provided important information about the limitations of single-fraction FLASH-RT that can be used in future trials designed to provide statistical evidence. In the cohort of canines with oral tumours, a high risk of osteoradionecrosis was found if bone was included in the treatment field. Around the same period, similar results were reported by Bley *et al.* in a randomized phase III trial in cat cancer patients with SCC (22). In that study, cats were randomly assigned to two arms; either 6 MV accelerated radiotherapy (2x4.8 Gy/day for 5 days) or 4.9 MeV FLASH-RT (single fraction of 34 Gy delivered in 3 pulses). At 9-15 months after treatment, 3/7 cats in the FLASH group developed maxillary bone necrosis and the study was terminated prematurely. This was the first publication to shed light on the challenges of FLASH single-fraction high-dose treatments, and the authors emphasized the need for caution and further investigation (22). The authors did a retrospective reconstruction of the dose distribution, which showed hot spots of 42 Gy in particular areas in the proximity of the bone.

Intensity-modulated electron FLASH radiotherapy

The revealed high risk of developing bone necrosis following high-dose single fraction FLASH-RT (22,105) were believed to be related to inhomogeneities in the dose distribution. Typical approaches used in CONV-RT to limit radiation-induced toxicity in normal tissue are to use homogeneous and conformal dose distributions with tight margins around the target volume. In **Paper IV**, bolus with uniform thickness was used to degrade the energy and limit the range of the electron beam in the tissue to avoid dose beyond the target. However, the PTV depth will vary across the tumour and will not match the penetration depth at all positions. In addition, complex surfaces, internal tissue heterogeneities, and air cavities may cause hot- and cold spots in the dose distribution leading to a nonuniform dose in the target volume,

underdosage of tumour and overdosage of normal tissue. To address these issues, the potential of intensity-modulated electron FLASH-RT in a clinical setting was evaluated in **Paper V**.

Intensity- and range-modulation

To increase the conformity in electron treatments, customized range-modulating bolus can be milled or 3D printed (106). This type of bolus spatially varies the electron beam energy based on the desired penetration depth. In the treatment planning system (TPS) used in **Paper V**, the research version of electronRT (.decimal, LCC, Sanford, Florida, USA), the option to create a CT-based variable thickness bolus is integrated. This bolus is designed so that the chosen therapeutic isodose (e.g., 90%) is conformed to the distal surface of the target volume. The system uses updated bolus design algorithms, based on those originally developed by Low et al. (107), which are used to generate an optimized bolus shape by applying bolus operators that create, modify, and extend the bolus. The creation operator forces the sum of the bolus thickness and physical depth of the planning target volume (PTV) to equal the therapeutic depth (e.g., R90) along each fan line from the virtual electron source that lies a certain distance inside the PTV. The modification operators (e.g., isodose shift, thickness smoothing, height smoothing, maximum PTV coverage) are added to refine the bolus design. The bolus thickness is then extended outside the collimator edge to take into account the dose contribution along the field edges. When the design is finished, the bolus can be ordered and subsequently fabricated by milling a block of machinable vax. Range-modulating bolus have been used clinically primarily for the treatment of postmastectomy chest wall to minimize lung and heart dose (106), and in head-and-neck cancer treatments to spare critical structures (108).

The irregular surface of the range-modulating bolus can cause a non-uniform dose distribution in the patient. Intensity-modulation, i.e., modulating the spatial distribution of the electron beam intensity, has been suggested as an option to minimize the loss in uniformity (106,109). In photon beam radiotherapy, intensity-modulation is performed using MLCs. However, due to the short treatment time associated with FLASH-RT, intensity-modulation using moving parts is not feasible. In addition, the air gap between the MLCs in a gantry head and the patient make this technique unsuitable for use in electron beams. Instead, Hogstrom *et al.* demonstrated the potential of passive intensity-modulation using a set of small island blocks of varying diameters located inside the electron block cut-out (109). The position and size of the island blocks are selected to deliver a desired intensity-modulated electron fluence distribution. The dose distribution resulting from the

bolus design is used to create an intensity-map, i.e., the maximum relative dose along each ray that goes through the PTV from a grid of points perpendicular to the beam central axis. Hogstrom *et al.* suggested that with island blocks of diameter d and separation r, in a hexagonal matrix, the reduced local intensity is given by:

$$I_{island\ blocks}(d,r) = I_0 \left[1 - \left(\frac{\pi}{2\sqrt{3}} \right) \left(\frac{d}{r} \right)^2 \right] \tag{12}$$

where I_0 is the intensity without island block (109). With a desired underlying intensity reduction factor at each point, $IRF = I_{desired}/I_0$, the block diameter for each point can be determined as:

$$d(r, IRF) = r \left[\left(\frac{2\sqrt{3}}{\pi} \right) (1 - IRF) \right]^{1/2} \tag{13}$$

In electronRT, the ability to utilize intensity-modulation according to the above method has been integrated. The intensity-modulation aperture is fabricated as 6 mm long cylindrical tungsten island blocks fixed in the electron block cut-out by embedding them in a low-density foam (109,110). The user sets a desired intensity, $I_{desired}$ (called IM factor in the TPS), whereafter the diameter of each island block that will most closely reduce the maximum ray line dose down to the provided IM factor is computed using an algorithm based on Eq. 14 (111). This way the intensity-modulation can be used to increase the homogeneity in the target volume by reducing hot spots (or increasing cold spots by lowering the relative dose everywhere else).

Treatment planning study in canine patients

A beam model of the 10 MeV UHDR electron beam of the clinical linear accelerator was created in electronRT and validated in a homogeneous solid water phantom using EBT-XD film measurements. In **Paper V**, the bolus and intensity-pin design and fabrication process (110) were first tested in a heterogeneous phantom with a 1 cm in diameter Styrofoam insert. Treatment plans were created with an open beam, with a range-modulating bolus and with a range-modulating bolus plus intensity-modulating pins with an IM factor of 0.8, and then the equipment was fabricated by the vendor. Once arrived, measurements were performed using EBT-XD film in a plane at 2 cm depth in the phantom. The results showed a good agreement between the measured and calculated 2D distribution, with a global gamma index 3%/3mm (with a threshold of 10% of the maximum dose) pass rate of ≥98% for all three scenarios. In the next step, a treatment planning study in canine patients was performed to evaluate intensity-modulated FLASH-RT in a clinical setting. For this

study (also reported in **Paper V**), simulated tumours were delineated in complex superficial head-and-neck areas, with bone and air cavities, to mimic some of the canine cases treated with FLASH-RT at the clinical linear accelerator. For each of the eight cases included, treatment plans were created with uniform bolus, uniform bolus plus intensity-modulation, range-modulating bolus, and range-modulating bolus plus intensity-modulation. Furthermore, the effect of varying the IM factor between 0.5 and 0.95 was investigated. Treatment plans were evaluated using a conformity index (CI), target dose homogeneity index (HI), maximum dose outside the target $D_{max,Body-PTV}$, and the minimum absorbed dose received by 98% of the volume, $D_{98\%}$, of the PTV (Table 2). Treatment plans were normalized so that 30 Gy was given as the median dose to the PTV.

Table 2. Dosimetric measures used for evaluation of treatment plans in Paper V. D_i is the minimum absorbed dose received by the i volume, V_{PTV} is the volume of the PTV and $V_{treated}$ is the volume enclosed by the minimum isodose in the PTV.

Dosimetry measure	Terminology/Definition
Conformity index	$CI = V_{PTV}/V_{treated}$
Target dose homogeniety index	$HI = (D_{2\%} - D_{98\%})/D_{50\%}$
Maximum dose outside target	$D_{max,Body-PTV}\ (Gy)$
Minimum dose received by 98% of the volume	$D_{98\%}\ (Gy)$

For statistical comparison of dosimetric measures between treatment plans, the paired Wilcoxon test with a chosen significance level of 5% was used. The results suggested that the HI could be significantly improved with the addition of intensity-modulation pins (IM factor=0.7), both when using a uniform bolus (p=0.017) and when using range-modulating bolus (p=0.028) (Figure 15). The use of range-modulating bolus improved the conformity of the treatment compared to using a uniform bolus, both when using bolus alone (p=0.046) and when using it in combination with intensity-modulation with IM factor=0.7 (p=0.018). To see a benefit of IM on HI, the IM factor had to be ≤0.8 for the uniform bolus and ≤0.9 for the range-modulating bolus. For the uniform bolus, an IM factor ≤0.8 also reduced the CI compared to bolus alone. However, for the range-modulating bolus, the CI was only reduced for highly modulated beams with IM factors ≤0.6. The median $D_{max,Body-PTV}$ decreased when using a range-modulating bolus as compared to uniform bolus, although not statistically significant. The $D_{98\%}$ of the PTV was >90% of the prescribed dose in 7/8 cases using range-modulating bolus, while with a uniform bolus the $D_{98\%}$ was <90%

in 4/8 cases. Figure 16 illustrates the transverse view of one of the canine cases with a simulated nasal tumour, for three different treatment plans; uniform bolus, uniform bolus with intensity-modulation, and range-modulating bolus with intensity-modulation.

From **Paper V** it was concluded that the target dose homogeneity in canine patients with complex heterogeneous tissue in the head-and-neck region could be improved by intensity-modulation. It was also concluded that range-modulating bolus could add an additional improvement in both target dose homogeneity and conformity. In future clinical electron FLASH-RT trials, we aim to use this technique to avoid hot spots in the dose distribution, which will hopefully lead to a reduced risk of severe radiation-induced toxicity. **Paper V** was the first evaluation of intensity-modulated FLASH-RT in complex areas of the head-and-neck with a lot of heterogeneities.
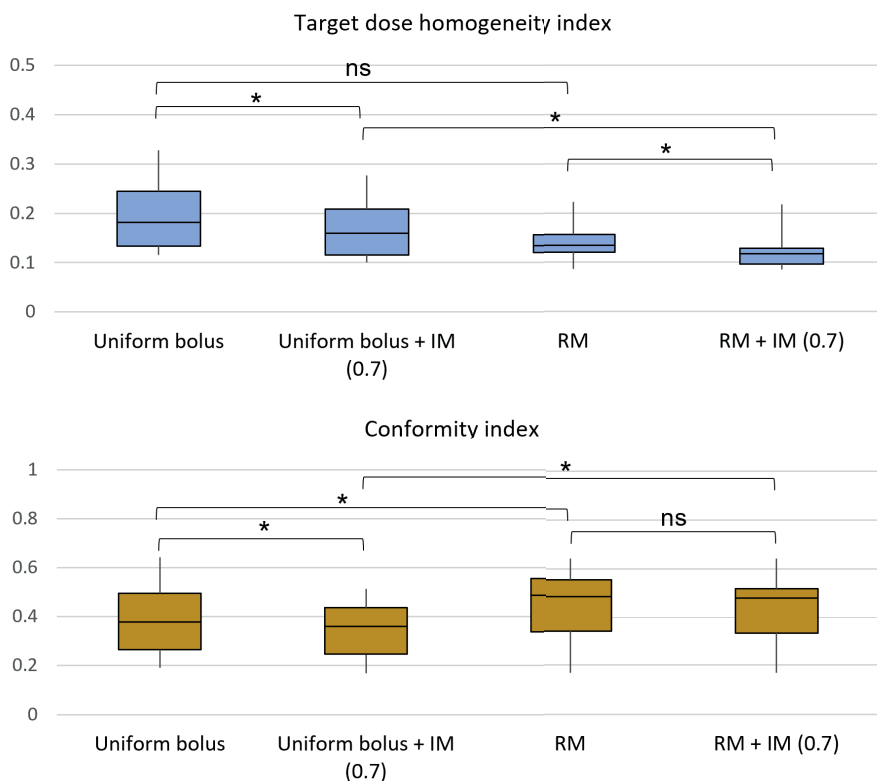
Figure 15: Box-plot of the distribution of target dose homogenity index and conformity index amongst the eight canine cases. * indicates significant difference (p≤0.05) using Wilcoxon rank sum-test.
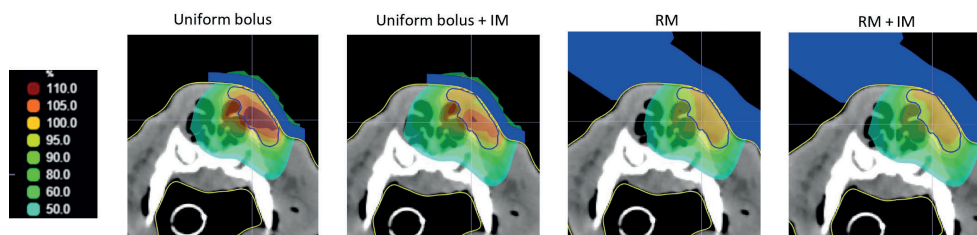
Figure 16: Dose distribution in transverse view for a canine with a simulated nasal tumour for four different treatment plan scenarios: uniform bolus, uniform bolus + intensity-modulation (IM, IM factor=0.7), range-modulation (RM), and RM+IM (IM factor=0.7). Treatment plans consists of a single electron beam, and were normalized so that the prescribed dose (30 Gy) was given as the median dose to the planning target volume, (PTV, deliniated in blue).

Discussion

Before moving forward with clinical trials in human patients, it will be important to investigate long-term effects of normal tissue in clinically relevant spontaneous tumours, such as those in veterinary patients. In these treatments, measures similar to those in CONV-RT must be taken to limit normal tissue toxicity. **Paper V** is the first study to investigate intensity-modulation of (FLASH) electron beams in highly heterogeneous tissue with bone and air cavities in the treatment field. The main conclusions drawn from **Paper V** are in line with previous studies on intensity-modulated electron therapy (106,110,112). Previous studies have demonstrated the potential of intensity-modulation for postmastectomy chest wall irradiation and temple, in cases with less heterogeneities than in the canine cases in **Paper V**. In addition, previous studies have been performed with medium to large field sizes, which will likely have a larger benefit of intensity-modulation due to the higher number of pins.

When using intensity-modulation for FLASH-RT, the fact that the tungsten pins will reduce the intensity of the electron beam has to be specially considered. If the IM factor is set to the same value as the lowest value in the intensity-map, tungsten pins will be added to all points with maximum dose along the ray line higher than that value, as an attempt to bring the entire dose field down to the minimum level. With a constant absolute dose normalization, the treatment time will have to be extended when the overall intensity is decreased. Although the beam parameters needed for a FLASH effect is not completely clear at this point, it must be ensured that the intensity is not reduced to a degree where the radiobiological benefit of FLASH is lost. With the lowest IM factor of 0.5 investigated in **Paper V**, the maximum decrease is intensity/dose rate would be 50%. With the current setup for treatment of canine

patients, a 50% reduction in dose rate would still allow for average dose rates of several hundreds of Gy/s.

The intensity-modulation feature is still under development in the TPS. One of the current main limitations (at least for highly heterogeneous cases) is the 1D approach to determine the position and diameter of the tungsten pins. This approach does not take into account hot spots created by lateral scatter in the tissue. It is rather intended for hot spots caused by the variable surface of the range-modulation bolus due to multiple Coulomb scattering or by an angled incidence that increase and/or decrease dose due to variations in SSD. Thus, for cases with a high level of heterogeneous tissue, an intensity-modulation approach that also considers lateral scatter may be more advantageous.

Clinical applications and trials

If the sparing effect of FLASH-RT can be reproduced in humans, it can be exploited in at least three ways: to reduce the toxicity of cancers where tumour control is already achieved with CONV-RT, to reduce the number of fractions without increasing toxicity, or to escalate the dose to radioresistant tumours that are difficult to cure, such as glioblastomas, without increasing toxicity. It may be administered as a separate treatment or as a boost to existing treatment schedules. The ultimate application of FLASH-RT in the clinic is currently unknown. The first studies on FLASH were performed using high-energy electrons and the first proof-of-concept in humans started in that setting (24,25). The limited penetration depth of high-energy electron beams makes them suitable for superficial lesions such as SCC, malignant melanoma, and subcutaneous T-cell lymphoma. These cancers are often developed in elderly patients and, if not amendable with surgery, requires a long series of radiotherapy treatments (24). FLASH-RT might allow for higher fraction doses and thus a reduced number of fractions, i.e., hypofractionated treatments schedules (27). Another setting where electron FLASH-RT could be beneficial is in IORT, where generally a single large dose is administered to the tumour during surgery (113).

The first human patient treated with electron FLASH-RT was reported in 2019 (24). More recently the results from the first clinical trial, FAST-01, using a transmission proton beam to treat bone metastasis of the extremities, were published (26). The aim of this trial was to demonstrate feasibility and safety. The FAST-02 trial is currently ongoing, including patients with bone metastasis in the thoracic region (114). The first-in-human clinical trial with electron FLASH-RT (IMPulse) is a phase I dose-escalation trial currently ongoing at CHUV in Lausanne (38). The study focuses on

controlling skin metastases from melanoma by delivering a single fraction of 22-34 Gy, with the primary aim to find the maximum tolerated dose for small and large lesions, respectively. Another trial in preparation at the CHUV is a randomized phase II trial of FLASH-RT versus CONV-RT for treatment of localized cutaneous SCC or basal cell carcinoma (39). Depending on the size of the lesion patients will receive either a single dose of 22 Gy or a fractionated dose of 5x6 Gy. The aim is to describe and compare the toxicity and efficacy of FLASH-RT versus CONV-RT.

Future perspectives

To reduce the risk of late toxicity in future veterinary and human head-and-neck electron FLASH treatments, one can either reduce the total dose, improve the dose distribution, or fractionate the treatment. With a reduced total dose, the efficacy of the treatment found in the cohort of canines with oral tumours might be lost, which is not desirable. If single fractions are still to be considered, homogeneous and conformal treatments are required to avoid hot spots and reduce unwanted dose outside the target. This was addressed in the treatment planning study in **Paper V**, where it was found that the target dose homogeneity and conformity of the treatment could be improved by intensity-modulation and range-modulation. In future canine treatments, intensity-modulation and range-modulation will be used to evaluate whether this approach can mitigate the normal tissue effects seen in previous single fraction high dose FLASH-RT treatments (22,105). However, it is also of high clinical importance to explore if FLASH-RT can be fractionated. Currently, only limited preclinical data exists on fractionated FLASH-RT schedules (27). Hypofractionation has been suggested as a potential clinical application for FLASH-RT given the current shift in CONV-RT towards more hypofractionated treatment regimens. Thus, future work will also aim to establish a clinical comparison of efficacy between single fraction and hypofractionated FLASH-RT. The first step will be to expand the previous work with a hypofractionated dose-escalation trial in canine patients, to find a treatment schedule with a comparable level of normal tissue complications as for the single fraction treatments.

A major limitation of the clinical electron FLASH studies conducted so far (except for the interrupted feline study) is the lack of a CONV-RT arm for comparison. To gain controlled evidence for the benefits of electron FLASH-RT, a randomized trial with FLASH-RT and CONV-RT would be ideal. However, the design of such a comparison is not straight-forward. If the trial is set up to investigate whether UHDR irradiation spares normal tissue compared to CONV dose rates, then a comparison

with equal particle type, prescribed dose, etc. for FLASH and CONV should be conducted. On the contrary, if the trial is set up to investigate whether FLASH-RT can improve radiotherapy treatments, a comparison with the current standard-of-care is more appropriate. However, a CONV-RT group receiving 16-20 fractions requires a lot of resources since a high number of patients will be needed to obtain meaningful statistics.

Conclusions

In the work covered in this thesis, we have promoted the clinical translation of FLASH-RT by developing and evaluating tools and procedures to measure, plan, and deliver an UHDR electron beam in a preclinical and clinical setting using a clinical linear accelerator.

In the first part, we investigated the potential of transmission chamber-based beam monitoring at UHDR. Transmission chambers are the golden standard for beam monitoring in clinical linear accelerators but generally suffer from large recombination effects in UHDR beams. We found that the charge collection efficiency in large plane-parallel transmission chambers could be increased by increasing the chamber voltage (**Paper I**) and reducing the electrode gap, and that the operating DPP range of the chamber could be extended up to the UHDR regimen (**Paper II**).

In the second part, we established procedures for preclinical and clinical irradiations in the UHDR electron beam. We developed setups and dosimetric procedures for accurate *in vitro* and *in vivo* irradiations (**Paper III**). These procedures are critical for performing high quality radiobiological experiments that can help understand the biological mechanisms underlying the observed FLASH effect, and guide the selection of conditions and beam parameters to test in clinical trials. We also established a workflow for clinical FLASH-RT in veterinary canine patients with spontaneous cancers and demonstrated the feasibility of FLASH-RT in clinically relevant scenarios (**Paper IV**). To avoid hot spots in future clinical trials, we evaluated a passive intensity-modulation technique that utilizes tungsten pins in the electron block cut-out, and we found that the homogeneity of the dose distribution could be improved compared to an open electron beam (**Paper V**).

Overall, the work in this thesis provides solutions to some of the critical issues encountered on the way towards a clinical translation of FLASH-RT. However, before a large-scale translation of FLASH-RT can be considered, further work is needed to solve the remaining technical and physical challenges, such as developing treatment machines capable of safe and accurate delivery of the prescribed dose to the patient.

Acknowledgements

I am proud to finally have completed this thesis. I may have gained a few wrinkles along the way, but it was all worth it. However, this thesis is not the result of my own genius and hard work alone, because I could not have done it without the support and encouragement from numerous people.

First of all, I want to thank Crister Ceberg. Not only did you keep me on track and guide me through this whole process, but you also made it all very fun and enjoyable. Thank you for believing in me. I feel lucky to have had you as my main supervisor!

To Kristoffer Petersson, who introduced me to the topic and has been a constant source of support and quick feedback. I could not have done it without you and all of your clever ideas. You have been a brilliant supervisor!

To Henrietta Nittby Redebrandt, my supervisor and a skilled neurosurgeon, thank you for being an inspiration and a source of energy during our many late evenings spent doing experiments.

To the former and current engineers at the Radiotherapy department at SUS involved in the FLASH project: Börje Blad, Andreas Thoft, Michael Lempart, and Pontus Wahlqvist, you have all been key players in making this work possible. And to the engineers Malin Spoelstra, Lars Andersson Ljus, Jan Hultkvist, Per Wendel, and others, who through fire and dust have kept the 20-year-old accelerator in shape. You are the real MVPs!

To my vet colleagues, Betina Børresen and Maja L. Arendt, thank you for showing me how we can do research and at the same time improve the quality of life for our furry companions.

To Sofie Ceberg, who encourage me to embark on this journey in the first place. I am very glad that you did. Thanks for all the laughs (especially during our trip to Quebec) and for always bringing joy to everyone around you.

To all the members of the Radiotherapy Physics group at Medical Radiation Physics, I am grateful for all support, feedback, and fruitful discussions. Special thanks to Annika Mannerberg for being a true companion during these years. After having

References

1.   Delaney G, Jacob S, Featherstone C, Barton M. The role of radiotherapy in cancer treatment: Estimating optimal utilization from a review of evidence-based clinical guidelines. Cancer. 2005;104(6):1129–37.
2.   Favaudon V, Caplier L, Monceau V, Pouzoulet F, Sayarath M, Fouillade C, et al. Ultrahigh dose-rate FLASH irradiation increases the differential response between normal and tumor tissue in mice. Sci Transl Med. 2014;6(245):245ra93.
3.   Wilson JD, Hammond EM, Higgins GS, Petersson K. Ultra-High Dose Rate (FLASH) Radiotherapy: Silver Bullet or Fool's Gold? Front Oncol. 2020;9:1563.
4.   Bourhis J, Montay-Gruel P, Gonçalves Jorge P, Bailat C, Petit B, Ollivier J, et al. Clinical translation of FLASH radiotherapy: Why and how? Radiotherapy and Oncology. 2019;139:11–7.
5.   Esplen N, Mendonca MS, Bazalova-Carter M. Physics and biology of ultrahigh dose-rate (FLASH) radiotherapy: A topical review. Phys Med Biol. 2020;65(23).
6.   Vozenin MC, Bourhis J, Durante M. Towards clinical translation of FLASH radiotherapy. Nat Rev Clin Oncol. 2022;19(December):791–803.
7.   Schüler E, Acharya M, Montay-Gruel P, Loo BW, Vozenin MC, Maxim PG. Ultra-high dose rate electron beams and the FLASH effect: From preclinical evidence to a new radiotherapy paradigm. Med Phys. 2022;49(3):2082–95.
8.   Dewey DL, Boag JW. Modification of the Oxygen Effect when Bacteria are given Large Pulses of Radiation. Nature. 1959;83:1450–1.
9.   Town CD. Effect of High Dose Rates on Survival of Mammalian Cells. Nature. 1967;215:847–8.
10. Hendry JH, Moore J V, Hodgson BW, Keene JP. The Constant Low Oxygen Concentration in All the Target Cells for Mouse Tail Radionecrosis. Radiat Res. 1982;92(1):172–81.
11. Epp ER, Weiss H, Santomasso A, Epp ER, Weiss H, Santomasso ANN. The Oxygen Effect in Bacterial Cells Irradiated with High-Intensity Pulsed Electrons. Radiation Research Society. 1968;34(2):320–5.

12. Field SB, Bewley DK. Effects of Dose-rate on the Radiation Response of Rat Skin. Int J Radiat Biol Relat Stud Phys Chem Med. 1974;26(3):259–67.

13. Hornsey S, Bewley DK. Hypoxia in Mouse Intestine Induced by Electron Irradiation at High Dose-rates. Int J Radiat Biol Relat Stud Phys, Chem Med. 1971;19(5):479–83.

14. Nias AHW, Swallow AJ, Keene JP, Hodgson BW. Survival of hela cells from 10 nanosecond pulses of electrons. Int J Radiat Biol. 1970;17(6):595–8.

15. Cygler J, Klassen N v., Ross CK, Bichay TJ, Raaphorst GP. The survival of aerobic and anoxic human glioma and melanoma cells after irradiation at ultrahigh and clinical dose rates. Radiat Res. 1994;140(1):79–84.

16. Zackrisson BU, Nystrom UH, Ostbergh P. Biological Response in Vitro To Pulsed High Dose Rate Electrons From A Clinical Accelerator. Acta Oncol (Madr). 1991;30(6):747–51.

17. Montay-Gruel P, Petersson K, Jaccard M, Boivin G, Germond JF, Petit B, et al. Irradiation in a flash: Unique sparing of memory in mice after whole brain irradiation with dose rates above 100Gy/s. Radiother Oncol. 2017;124(3):365–9.

18. Vozenin MC, Hendry JH, Limoli CL. Biological Benefits of Ultra-high Dose Rate FLASH Radiotherapy: Sleeping Beauty Awoken. Clin Oncol. 2019;31(7):407–15.

19. Borghini A, Vecoli C, Labate L, Panetta D, Andreassi MG, Gizzi LA. FLASH ultra-high dose rates in radiotherapy: preclinical and radiobiological evidence. Int J Radiat Biol. 2021;98(2):127–35.

20. Böhlen TT, Germond JF, Bourhis J, Vozenin MC, Ozsahin EM, Bochud F, et al. Normal Tissue Sparing by FLASH as a Function of Single-Fraction Dose: A Quantitative Analysis. Int J Radiat Oncol Biol Phys. 2022;114(5):1032–44.

21. Vozenin MC, De Fornel P, Petersson K, Favaudon V, Jaccard M, Germond JF, et al. The Advantage of FLASH Radiotherapy Confirmed in Mini-pig and Cat-cancer Patients. Clinical Cancer Research. 2019;25(1):35–42.

22. Bley CR, Wolf F, Jorge PG, Grilj V, Petridis I, Petit B, et al. Dose- And Volume-Limiting Late Toxicity of FLASH Radiotherapy in Cats with Squamous Cell Carcinoma of the Nasal Planum and in Mini Pigs. Clinical Cancer Research. 2022;28(17):3814–23.

23. Velalopoulou A, Karagounis I V, Cramer GM, Kim MM, Skoufos G, Goia D, et al. FLASH Proton Radiotherapy Spares Normal Epithelial and Mesenchymal Tissues While Preserving Sarcoma Response. Cancer Res. 2021;(7):4808–22.

24. Bourhis J, Sozzi WJ, Jorge PG, Gaide O, Bailat C, Duclos F, et al. Treatment of a first patient with FLASH-radiotherapy. Radiotherapy and Oncology. 2019 Oct;139:18–22.

25. Gaide O, Herrera F, Jeanneret Sozzi W, Gonçalves Jorge P, Kinj R, Bailat C, et al. Comparison of ultra-high versus conventional dose rate radiotherapy in a patient with cutaneous lymphoma. Radiotherapy and Oncology. 2022 Sep;174:87–91.

26. Mascia AE, Daugherty EC, Zhang Y, Lee E, Xiao Z, Sertorio M, et al. Proton FLASH Radiotherapy for the Treatment of Symptomatic Bone Metastases The FAST-01 Nonrandomized Trial. JAMA Oncol. 2022;0757:1–7.

27. Montay-Gruel P, Acharya MM, Jorge PG, Petit B, Petridis IG, Fuchs P, et al. Hypofractionated FLASH-RT as an effective treatment against glioblastoma that reduces neurocognitive side effects in mice. Clinical Cancer Research. 2021;27(3):775–84.

28. Lansonneur P, Favaudon V, Heinrich S, Fouillade C, Verrelle P, De Marzi L. Simulation and experimental validation of a prototype electron beam linear accelerator for preclinical studies. Physica Medica. 2019 Apr 1;60:50–7.

29. Jaccard M, Duran MT, Petersson K, Germond JF, Liger P, Vozenin MC, et al. High dose-per-pulse electron beam dosimetry: Commissioning of the Oriatron eRT6 prototype linear accelerator for preclinical use. Med Phys. 2018;45(2):863–74.

30. Petersson K, Jaccard M, Germond JF, Buchillier T, Bochud F, Bourhis J, et al. High dose-per-pulse electron beam dosimetry - A model to correct for the ion recombination in the Advanced Markus ionization chamber. Med Phys. 2017;44(3):1157–67.

31. Schüler E, Trovati S, King G, Lartey F, Rafat M, Villegas M, et al. Experimental Platform for Ultra-high Dose Rate FLASH Irradiation of Small Animals Using a Clinical Linear Accelerator. Int J Radiat Oncol Biol Phys. 2017;97(1):195–203.

32. Lempart M, Blad B, Adrian G, Back S, Knoos T, Ceberg C, et al. Modifying a clinical linear accelerator for delivery of ultra-high dose rate irradiation. Radiother Oncol [Internet]. 2019; Available from: https://www.ncbi.nlm.nih.gov/pubmed/30755324

33. Rahman M, Ashraf MR, Zhang R, Bruza P, Dexter CA, Thompson L, et al. Electron FLASH Delivery at Treatment Room Isocenter for Efficient Reversible Conversion of a Clinical LINAC. Int J Radiat Oncol Biol Phys. 2021;110(3):872–82.

34. Felici G, Barca P, Barone S, Bortoli E, Borgheresi R, de Stefano S, et al. Transforming an IORT Linac Into a FLASH Research Machine: Procedure and Dosimetric Characterization. Front Phys. 2020;8(September):1–11.

35. Di Martino F, Barca P, Barone S, Bortoli E, Borgheresi R, De Stefano S, et al. FLASH Radiotherapy With Electrons: Issues Related to the Production, Monitoring, and Dosimetric Characterization of the Beam. Front Phys. 2020;8(November):1–14.

36. Giuliano L, Franciosini G, Palumbo L, Aggar L, Dutreix M, Faillace L, et al. Characterization of Ultra-High-Dose Rate Electron Beams with ElectronFlash Linac. Appl Sci. 2023;13(1):631.

37. Moeckli R, Gonçalves Jorge P, Grilj V, Oesterle R, Cherbuin N, Bourhis J, et al. Commissioning of an ultra-high dose rate pulsed electron beam medical LINAC for FLASH RT preclinical animal experiments and future clinical human protocols. Med Phys. 2021;48(6):3134–42.

38. ClinicalTrials.gov [Internet]. Bethesda (MD): National Library of Medicine (US). 2000 Feb 29 - . Identifier NCT04986696, Irradiation of Melanoma in a Pulse (IMPulse); 2021 Aug 3. [cited 2023 Mar 23]. Available from: https://clinicaltrials.gov/ct2/show/NCT04986696

39. ClinicalTrials.gov [Internet]. Bethesda (MD): National Library of Medicine (US). 2000 Feb 29 - . Identifier NCT05724875, FLASH Radiotherapy for Skin Cancer (LANCE); 2023 Feb 13. [cited 2023 Mar 23]. Available from: https://clinicaltrials.gov/ct2/show/NCT05724875

40. Patriarca A, Fouillade C, Auger M, Martin F, Pouzoulet F, Nauraye C, et al. Experimental Set-up for FLASH Proton Irradiation of Small Animals Using a Clinical System. Int J Radiat Oncol Biol Phys. 2018;102(3):619–26.

41. Diffenderfer ES, Verginadis II, Kim MM, Shoniyozov K, Velalopoulou A, Goia D, et al. Design, Implementation, and in Vivo Validation of a Novel Proton FLASH Radiation Therapy System. Int J Radiat Oncol Biol Phys. 2020;106(2):440–8.

42. Titt U, Yang M, Wang X, Iga K, Fredette N, Schueler E, et al. Design and validation of a synchrotron proton beam line for FLASH radiotherapy preclinical research experiments. Med Phys. 2022 Jan 1;49(1):497–509.

43. Darafsheh A, Hao Y, Zwart T, Wagner M, Catanzano D, Williamson JF, et al. Feasibility of proton FLASH irradiation using a synchrocyclotron for preclinical studies. Med Phys. 2020 Sep 1;47(9):4348–55.

44. Darafsheh A, Hao Y, Zhao X, Zwart T, Wagner M, Evans T, et al. Spread-out Bragg peak proton FLASH irradiation using a clinical synchrocyclotron: Proof of concept and ion chamber characterization. Med Phys. 2021 Aug 1;48(8):4472–84.

45. Jolly S, Owen H, Schippers M, Welsch C. Technical challenges for FLASH proton therapy. Physica Medica. 2020;78(January):71–82.

46. Wei S, Lin H, Shi C, Xiong W, Chen CC, Huang S, et al. Use of single-energy proton pencil beam scanning Bragg peak for intensity-modulated proton therapy FLASH treatment planning in liver-hypofractionated radiation therapy. Med Phys. 2022 Oct 1;49(10):6560–74.

47. Gao F, Yang Y, Zhu H, Wang J, Xiao D, Zhou Z, et al. First demonstration of the FLASH effect with ultrahigh dose rate high-energy X-rays. Radiotherapy and Oncology. 2022;166:44–50.

48. Montay-Gruel P, Bouchet A, Jaccard M, Patin D, Serduc R, Aim W, et al. X-rays can trigger the FLASH effect: Ultra-high dose-rate synchrotron light source prevents normal brain injury after whole brain irradiation in mice. Radiotherapy and Oncology. 2018;129(3):582–8.

49. Bazalova-Carter M, Esplen N. On the capabilities of conventional x-ray tubes to deliver ultra-high (FLASH) dose rates. Med Phys. 2019;46(12):5690–5.

50. Maxim PG, Tantawi SG, Loo BW. PHASER: A platform for clinical translation of FLASH cancer radiotherapy. Radiotherapy and Oncology. 2019;139:28–33.

51. Bazalova-Carter M, Qu B, Palma B, Hårdemark B, Hynning E, Jensen C, et al. Treatment planning for radiotherapy with very high-energy electron beams and comparison of VHEE and VMAT plans. Med Phys. 2015;42(5):2615–25.

52. DesRosiers C, Moskvin V, Bielajew A, Papiez L. 150-250 MeV electron beams in radiation therapy. Phys Med Biol. 2000;(45):1781–805.

53. Karlsson M, Nyström H, Svensson H. Electron beam characteristics of the 50-MeV racetrack microtron. Med Phys [Internet]. 1992 Mar 1 [cited 2023 May 2];19(2):307–15. Available from: https://onlinelibrary.wiley.com/doi/full/10.1118/1.596933

54. Hooker SM. Developments in laser-driven plasma accelerators. Nat Photonics. 2013;7(10):775–82.

55. Peralta EA, Soong K, England RJ, Colby ER, Wu Z, Montazeri B, et al. Demonstration of electron acceleration in a laser-driven dielectric microstructure. Nature. 2013;503:91–4.

56. Schüller A, Heinrich S, Fouillade C, Subiel A, Marzi L De, Romano F, et al. The European Joint Research Project UHDpulse – Metrology for advanced radiotherapy using particle beams with ultra-high pulse dose rates. Physica Medica. 2020;80(January):134–50.

57. Technical report series 398. Absorbed Dose Determination in External Beam Radiotherapy: An International Code of Practice for Dosimetry based on

Standard of Absorbed Dose to Water. International Atomic Energy Agency. Vienna; 2000.

58.   Burns DT, McEwen MR. Ion recombination corrections for the NACP parallel-plate chamber in a pulsed electron beam. Phys Med Biol. 1998;43(8):2033–45.

59.   Boag JW, Hochhäuser E, Balk OA. The effect of free-electron collection on the recombination correction to ionization measurements of pulsed radiation. Phys Med Biol. 1996;41(5):885–97.

60.   Gotz M, Karsch L, Pawelke J. A new model for volume recombination in plane-parallel chambers in pulsed fields of high dose-per-pulse. Phys Med Biol. 2017;62(22):8634–54.

61.   Sutton JD, Littler JP. Accounting for the ion recombination factor in relative dosimetry of flattening filter free photon radiation. Biomed Phys Eng Express. 2017 Jan;3(1):017002.

62.   Boag JW, Wilson T. The saturation curve at high ionization intensity. Br J Appl Phys. 1952;3:222–9.

63.   Smyth LML, Donoghue JF, Ventura JA, Livingstone J, Bailey T, Day LRJ, et al. Comparative toxicity of synchrotron and conventional radiation therapy based on total and partial body irradiation in a murine model. Sci Rep. 2018;8(1):12044.

64.   Beyreuther E, Brand M, Hans S, Hidegehéty K, Karsch L, Leßmann E, et al. Feasibility of proton FLASH effect tested by zebrafish embryo irradiation. Radiotherapy and Oncology. 2019;139:46–50.

65.   Kranzer R, Poppinga D, Weidner J, Schüller A, Hackel T, Looe HK, et al. Ion collection efficiency of ionization chambers in ultra-high dose-per-pulse electron beams. Med Phys. 2021;48(2):819–30.

66.   Gómez F, Gonzalez-Castaño DM, Fernández NG, Pardo-Montero J, Schüller A, Gasparini A, et al. Development of an ultra-thin parallel plate ionization chamber for dosimetry in FLASH radiotherapy. Med Phys. 2022;49(7):4705–14.

67.   Kranzer R, Andreas Schüller, Faustino Gomez Rodriguez, Weidner J, Paz-Martín J, Looe HK, et al. Charge collection efficiency , underlying recombination mechanisms , and the role of electrode distance of vented ionization chambers under ultra-high dose-per-pulse conditions. Physica Medica. 2022;104(November):10–7.

68.   Di Martino F, Del Sarto D, Giuseppina Bisogni M, Capaccioli S, Galante F, Gasperini A, et al. A new solution for UHDP and UHDR (Flash) measurements: Theory and conceptual design of ALLS chamber. Physica Medica. 2022 Oct 1;102:9–18.

69. Almond PR, Biggs PJ, Coursey BM, Hanson WF, Huq MS, Nath R, et al. AAPM's TG-51 protocol for clinical reference dosimetry of high-energy photon and electron beams. Med Phys. 1999;26(9):1847–70.

70. Boag JW, Hochhauser E, Balk OA. The effect of free-electron collection on the recombination correction to ionization measurements of pulsed radiation. Phys Med Biol. 1996;41(5):885–97.

71. Laitano RF, Guerra AS, Pimpinella M, Caporali C, Petrucci A. Charge collection efficiency in ionization chambers exposed to electron beams with high dose per pulse. Phys Med Biol. 2006;51(24):6419–36.

72. Burns JE, Burns DT. Comments on Ion Recombination Corrections for Plane-Parallel and Thimble Chambers in Electron and Photon Radiation. Phys Med Biol. 1993;38(12):1986–8.

73. Bruggmoser G, Saum R, Schmachtenberg A, Schmid F, Schüle E. Determination of the recombination correction factor kS for some specific plane-parallel and cylindrical ionization chambers in pulsed photon and electron beams. Phys Med Biol. 2007;52(2).

74. Cavallone M, Bailat C, Jorge PG, Moeckli R, Delorme R, Flacco A, et al. Determination of the ion collection efficiency of the Razor Nano Chamber for ultra-high dose-rate electron beams. Med Phys. 2022;49:4731–42.

75. Niroomand-Rad A, Chiu-Tsao ST, Grams MP, Lewis DF, Soares CG, Van Battum LJ, et al. Report of AAPM Task Group 235 Radiochromic Film Dosimetry: An Update to TG-55. Med Phys. 2020;47(12):5986–6025.

76. Jorge PG, Jaccard M, Petersson K, Gondré M, Durán MT, Desorgher L, et al. Dosimetric and preparation procedures for irradiating biological models with pulsed electron beam at ultra-high dose-rate. Radiotherapy and Oncology. 2019;139:34–9.

77. Jaccard M, Petersson K, Buchillier T, Germond JF, Duran MT, Vozenin MC, et al. High dose-per-pulse electron beam dosimetry: Usability and dose-rate independence of EBT3 Gafchromic films. Med Phys. 2017;44(2):725–35.

78. Livingstone J, Stevenson AW, Butler DJ, Hausermann D, Adam JF. Characterization of a synthetic single crystal diamond detector for dosimetry in spatially fractionated synchrotron x-ray fields. Med Phys. 2016;43(7):4283.

79. Kranzer R, Schüller A, Bourgouin A, Hackel T, Poppinga D, Lapp M, et al. Response of diamond detectors in ultra-high dose-per-pulse electron beams for dosimetry at FLASH radiotherapy. Phys Med Biol. 2022;67(7).

80. Marinelli M, Felici G, Galante F, Gasparini A, Giuliano L, Heinrich S, et al. Design, realization, and characterization of a novel diamond detector prototype for FLASH radiotherapy dosimetry. Med Phys. 2022;49(3):1902–10.

81. Verona Rinati G, Felici G, Galante F, Gasparini A, Kranzer R, Mariani G, et al. Application of a novel diamond detector for commissioning of FLASH radiotherapy electron beams. Med Phys. 2022 Aug 1;49(8):5513–22.

82. Karsch L, Beyreuther E, Burris-Mog T, Kraft S, Richter C, Zeil K, et al. Dose rate dependence for different dosimeters and detectors: TLD, OSL, EBT films, and diamond detectors. Med Phys. 2012;39(5):2447–55.

83. Kudoh H, Celina M, Kaye RJ, Gillen KT, Clough RL. Response of alanine dosimeters at very high dose rate. Applied Radiation and Isotopes. 1997 Apr;48(4):497–9.

84. Deene Y de. Essential characteristics of polymer gel dosimeters. J Phys Conf Ser. 2004;3:34–57.

85. Favaudon V, Lentz JM, Heinrich S, Patriarca A, de Marzi L, Fouillade C, et al. Time-resolved dosimetry of pulsed electron beams in very high dose-rate, FLASH irradiation for radiotherapy preclinical studies. Nucl Instrum Methods Phys Res A. 2019;944(August):162537.

86. Ashraf MR, Rahman M, Zhang R, Williams BB, Gladstone DJ, Pogue BW, et al. Dosimetry for FLASH Radiotherapy: A Review of Tools and the Role of Radioluminescence and Cherenkov Emission. Front Phys. 2020;8(August):1–20.

87. Beddar AS, Mackie TR, Attix FH. Water-equivalent plastic scintillation detectors for high-energy beam dosimetry: I. Physical characteristics and theoretical considerations. Phys Med Biol. 1992;37(10):1883.

88. Beddar AS, Mackie TR, Attix FH. Water-equivalent plastic scintillation detectors for high-energy beam dosimetry: II. Properties and measurements. Phys Med Biol. 1992;37(10):1901.

89. Beaulieu L, Beddar S. Review of plastic and liquid scintillation dosimetry for photon, electron, and proton therapy. Phys Med Biol. 2016;61(20):R305–43.

90. Rahman M, Ashraf MR, Zhang R, Gladstone DJ, Cao X, Williams BB, et al. Spatial and temporal dosimetry of individual electron FLASH beam pulses using radioluminescence imaging. Phys Med Biol. 2021;66(13).

91. Adrian G, Konradsson E, Lempart M, Bäck S, Ceberg C, Petersson K. The FLASH effect depends on oxygen concentration. Br J Radiol. 2019;(August):20190702.

92. Adrian G, Konradsson E, Beyer S, Wittrup A, Butterworth KT, McMahon SJ, et al. Cancer Cells Can Exhibit a Sparing FLASH Effect at Low Doses Under Normoxic In Vitro-Conditions. Front Oncol. 2021;11(July):1–9.

93. Di Martino F, Giannelli M, Traino AC, Lazzeri M. Ion recombination correction for very high dose-per-pulse high-energy electron beams. Med Phys. 2005;32(7):2204–10.

94. Kudoh H, Celina M, Kaye RJ, Gillen KT, Clough RL. Response of alanine dosimeters at very high dose rate. Applied Radiation and Isotopes. 1997;48(4):497–9.

95. McManus M, Romano F, Lee ND, Farabolini W, Gilardi A, Royle G, et al. The challenge of ionisation chamber dosimetry in ultra-short pulsed high dose-rate Very High Energy Electron beams. Sci Rep. 2020;10(1):1–16.

96. Gonçalves Jorge P, Grilj V, Bourhis J, Vozenin MC, Germond JF, Bochud F, et al. Technical note: Validation of an ultrahigh dose rate pulsed electron beam monitoring system using a current transformer for FLASH preclinical studies. Med Phys. 2022;49(3):1831–8.

97. Oesterle R, Gonçalves Jorge P, Grilj V, Bourhis J, Vozenin MC, Germond JF, et al. Implementation and validation of a beam-current transformer on a medical pulsed electron beam LINAC for FLASH-RT beam monitoring. J Appl Clin Med Phys. 2021;22(11):165–71.

98. Liu K, Palmiero A, Chopra N, Velasquez B, Li Z, Beddar S, et al. Dual beam-current transformer design for monitoring and reporting of electron ultra-high dose rate (FLASH) beam parameters. J Appl Clin Med Phys. 2023;24(2):e13891.

99. Pawelke, J., Brand, M., Hans, S., Hideghéty, K., Karsch, L., Lessmann, E., Löck, S., Schürer, M., Rita Szabó, E., Beyreuther E. Electron dose rate and oxygen depletion protect zebrafish embryo from radiation damage. Radiother Oncol. 2021;158:7–12.

100. Konradsson E, Liljedahl E, Gustafsson E, Adrian G, Beyer S, Ilaahi SE, et al. Comparable Long-Term Tumor Control for Hypofractionated FLASH Versus Conventional Radiation Therapy in an Immunocompetent Rat Glioma Model. Adv Radiat Oncol. 2022 Nov 1;7(6):101011.

101. Liljedahl E, Konradsson E, Gustafsson E, Jonsson KF, Olofsson JK, Ceberg C, et al. Long-term anti-tumor effects following both conventional radiotherapy and FLASH in fully immunocompetent animals with glioblastoma. Scientific Reports 2022 12:1. 2022 Jul 19;12(1):1–12.

102. Seyhan AA. Lost in translation: the valley of death across preclinical and clinical divide – identification of problems and overcoming obstacles. Transl Med Commun. 2019;4(1):1–19.

103. Björk P, Knöös T, Nilsson P, Larsson K. Design and dosimetry characteristics of a soft-docking system for intraoperative radiation therapy. Int J Radiat Oncol Biol Phys. 2000;47(2):527–33.

104. Konradsson E, Arendt ML, Jensen KB, Thomasson H, Børresen B, Petersson K, et al. Intracavitary Electron FLASH Radiotherapy in a Canine Cancer

Patient With Oral Malignant Melanoma. Int J Radiat Oncol Biol Phys. 2021;111(3):S31.

105. Børresen B, Arendt ML, Konradsson E, Jensen KB, Bäck S, Munck af Rosenschöld P, et al. Toxicity and efficacy of single-fraction high dose FLASH radiotherapy in a cohort of dogs with spontaneous malignant oral tumors. Submitted to Int J Radiat Oncol Biol Phys.

106. Kudchadker RJ, Hogstrom KR, Garden AS, McNeese MD, Boyd RA, Antolak JA. Electron conformal radiotherapy using bolus and intensity modulation. Int J Radiat Oncol Biol Phys. 2002;53(4):1023–37.

107. Low DA, Starkschall G, Buinowski SW, Wang LL, Hogstrom KR. Electron Bolus Design for Radiotherapy Treatment Planning: Bolus Design Algorithms. Vol. 19, Medical Physics. 1992. p. 115–24.

108. Kudchadker RJ, Antolak JA, Morrison WH, Wong PF, Hogstrom KR. Utilization of custom electron bolus in head and neck radiotherapy. J Appl Clin Med Phys. 2003;4(4):321–33.

109. Hogstrom KR, Carver RL, Chambers EL, Erhart K. Introduction to passive electron intensity modulation. J Appl Clin Med Phys. 2017;18(6):10.

110. Hilliard EN, Carver RL, Chambers EL, Kavanaugh JA, Erhart KJ, McGuffey AS, et al. Planning and delivery of intensity modulated bolus electron conformal therapy. J Appl Clin Med Phys. 2021 Oct 1;22(10):8–21.

111. Chambers EL. Design of a Passive Intensity Modulation Device for Bolus Electron Conformal Therapy [Internet] [Master's thesis]. Louisiana State University, Baton Rouge, LA; 2016. Available from: https://digitalcommons.lsu.edu/gradschool_theses/4384/

112. Doiron J. Benefit of Intensity Modulated Bolus Electron Conformal Therapy for Post Mastectomy Chest Wall [MS Thesis]. Louisiana State University and Agricultural and Mechanical College; 2018.

113. Calvo FA, Serrano J, Cambeiro M, Aristu J, Asencio JM, Rubio I, et al. Intra-Operative Electron Radiation Therapy: An Update of the Evidence Collected in 40 Years to Search for Models for Electron-FLASH Studies. Cancers (Basel). 2022;14(15).

114. ClinicalTrials.gov [Internet]. Bethesda (MD): National Library of Medicine (US). 2000 Feb 29 - . Identifier NCT05524064, FLASH Radiotherapy for the Treatment of Symptomatic Bone Metastases in the Thorax (FAST-02); 2022 Sep 1. [cited 2023 Mar 23]. Available from: https://clinicaltrials.gov/ct2/show/NCT05524064

Radiotherapy in a FLASH

FLASH radiotherapy involves treatment with an ultra-high dose rate (i.e., absorbed dose per unit of time), which is about 1000 times faster than what is currently used in clinical practice. This technique has the potential to protect normal tissue while maintaining the treatment effect and could present a considerable advancement in the field of radiotherapy. However, the short treatment times (less than a second) pose unique physical and technical challenges that need to be solved before implementing this technique in the clinic on a large scale.

This book is the doctoral thesis of Elise Konradsson and aims to address some of these challenges and promote the clinical translation of FLASH radiotherapy with electrons.

LUND
UNIVERSITY

9 789180 396660